

Data-Driven Safe Output Regulation of Strict-Feedback Linear Systems with Input Delay

Zhenxu Zhao, Ji Wang, Weiyao Lan

Abstract—This paper develops a data-driven safe control framework for linear systems possessing a known strict-feedback structure, but with most plant parameters, external disturbances, and input delay being unknown. By leveraging Koopman operator theory, we utilize Krylov dynamic mode decomposition (DMD) to extract the system dynamics from measured data, enabling the reconstruction of the system and disturbance matrices. Concurrently, the batch least-squares identification (BaLSI) method is employed to identify other unknown parameters in the input channel. Using control barrier functions (CBFs) and backstepping, we first develop a full-state safe controller. Based on this, we build an output-feedback controller by performing system identification using only the output data and actuation signals as well as constructing an observer to estimate the unmeasured plant states. The proposed approach achieves: 1) finite-time identification of a substantial set of unknown system quantities, and 2) exponential convergence of the output state (the state furthest from the control input) to a reference trajectory while rigorously ensuring safety constraints. The effectiveness of the proposed method is demonstrated through a safe vehicle platooning application.

Index Terms—Data-driven control, safe control, output regulation, input delay, Koopman operator, dynamic mode decomposition

I. INTRODUCTION

A. Output Regulation

Output regulation, which achieves asymptotic tracking of reference trajectories and disturbance rejection, has long been an important topic in control theory. As the fundamental work, Internal Model Principle (IMP) was first established in [21] for linear systems, which incorporates an exosystem model into the feedback controller. The work in [27] then extended this to the nonlinear dynamics by deriving the regulator equations, and a general framework was developed in [24], [25]. In addition to ODE systems, output regulation has also been studied for PDEs [26], [42]. A trajectory tracking result, based on a backstepping design, was presented in [9], which considered an ODE with unknown input delay—a problem closely related to hyperbolic PDEs. Article [3] addressed in-domain point outputs, later expanding to heterodirectional systems with constant coefficients [4], and [13], [14] further generalized this to spatially varying coefficients, establishing a link between the control design and regulator equations

Z. Zhao, J. Wang, W. Lan are with Department of Automation, Xiamen University, Xiamen 361005, China. (E-mail addresses: zhaozhenxu@stu.xmu.edu.cn (Z. Zhao), jiwang@xmu.edu.cn (J. Wang), wylan@xmu.edu.cn (W. Lan).)

based on output localization. In parallel, some results have been obtained for parabolic PDEs. The work in [34] combined backstepping and flatness approaches to design an output-tracking boundary controller. Similarly, [12] addressed output regulation for boundary-controlled PDEs subject to disturbances on both the domain and the uncontrolled boundary. The scope of this research has further expanded to include cooperative output-tracking problems involving time-varying structures [16], [18].

B. Safety-Critical Control in Complex Environments

Ensuring safety is a primary requirement in modern autonomous systems [1], [51], where one must rigorously guarantee that system trajectories remain within a prescribed safe set. Control Barrier Functions (CBFs) formalize this requirement via synthesizing safety filters through Quadratic Programs (QPs) [1], [2]. Practical deployment challenges have driven increasing research into CBF methods under complex real-world conditions. One of the most critical challenges arises from the presence of time delays, which can destabilize the system or invalidate safety filters, even when the delay is small [37], [51]. Recent work [51] integrates predictor feedback into CBF designs, using high-relative-degree CBFs [38], [50] rooted in non-overshooting techniques [31] to ensure safety under arbitrary-length delays. External disturbances pose another significant threat to safety, particularly in output-feedback settings complicated by state estimation errors. Notably, the work in [48] addressed this for PDE systems with full disturbances, establishing a framework that guarantees both exponential regulation and safety constraints.

However, the above approaches typically assume full knowledge of the system model, whereas real-world systems often contain substantial uncertainties. Robust CBF methods [28], [30] address such uncertainties by enforcing safety under worst-case conditions, but this inevitably leads to conservative designs. Adaptive Control Barrier Functions (aCBFs) were introduced in [43], drawing an analogy to adaptive Control Lyapunov Functions (aCLFs) to handle systems with parametric uncertainty. The aCBF methodology generally combines a parameter-adaptation law with a robust CBF constraint, but safety is ensured only by restricting the state to a strict subset of the nominal safe set, which remains conservative. More recently, the BaLSI adaptive safe control scheme in [47] significantly reduces conservatism by ensuring that, despite uncertainties, the system state returns to and remains within the original safe set after a finite transient. Nonetheless, these

methods still assume that only a small number of parameters are unknown, limiting their applicability in scenarios where the system model is entirely unavailable.

C. Data driven with DMD and Koopman operator

This gap becomes even more pronounced in many engineering applications, where first-principles modeling is infeasible due to complex or poorly understood physics [10], [23]. Consequently, data-driven control frameworks [6], [11], which extract dynamic models directly from time-series data to design controller that ensures closed-loop stability, have become essential. Data-driven methods, including Willems' fundamental lemma [39], [49] and informativity theory [45], have been highly effective for discrete-time linear systems, extending these to continuous-time settings remains challenging [41]. Koopman operator theory [7], [33] addresses this by lifting nonlinear dynamics into an infinite-dimensional observable space where the evolution becomes linear [35], offering a powerful data-driven framework even for LTI systems with disturbances [17]. Dynamic Mode Decomposition (DMD) [32], [40] provides practical Koopman approximations and has shown strong performance in system identification and flow control, though its standard one-step form is noise-sensitive and requires full-state data. Viewed through numerical linear algebra, DMD is closely linked to Krylov subspace methods [5], [19]. Since system data naturally form Krylov sequences, this connection enables Krylov DMD to construct observable bases via Hankel matrices and extract Koopman modes and eigenvalues more robustly.

The classical output regulation problem has only recently been explored from a purely data-driven perspective [22], [44], [53]. A pioneering study [17] used the Koopman operator and Krylov DMD to solve the regulator equations directly from data, thereby bypassing explicit parameter identification. However, this approach does not incorporate safety constraints that are indispensable in practical applications.

While data-driven control provides a powerful paradigm for stabilizing systems with unknown dynamics, establishing rigorous safety guarantees, which are crucial in practical applications, remains largely unresolved, with limited progress to date [8], [20], [36], [52]. Article [8] maintains the state within an invariant polyhedral set robustly using both model-based and date-driven approach. Recent work [52] employs a safely probabilistic framework under Gaussian noise with unknown covariance, while [36] develops a semi-definite programming approach to ensure safety against unknown bounded disturbances. Most existing approaches are constrained by intensive offline verification, high online computational costs, and a focus on discrete-time settings that neglect the impact of input delays. These challenges limit their applicability in practice and motivate the work presented in this paper.

D. Main contributions

In this paper, we develop a data-driven CBF-based safe control scheme for linear strict-feedback systems with significant model uncertainties, unknown external disturbances, and unknown input delay. The main contributions of this work are:

- 1) Compared with data-driven output regulation results [17], [53], we address a more challenging case where the plant is subject to unknown input delay and safety constraints.
- 2) Unlike recent safe adaptive methods [47], [51], which address only a small set of unknown parameters, the present work addresses a setting in which nearly the entire plant, including disturbances and input delays, is unknown, and moreover achieves safe output regulation solely using measurable output signals.
- 3) In contrast to recent data-driven safe control methods [8], [52], we develop a CBF-based controller for continuous-time systems with unknown input delays, removing the assumptions for bounds of unknown external disturbances and for the rank of data matrices.
- 4) To the best of our knowledge, this is the first result of data-driven safe control based on CBF with the Koopman operator and Krylov DMD, even if the input delay is excluded.

E. Organization

The problem is formulated in Sec. II. In Sec. III, we present the identification of all unknown parameters and the data-driven safe control design under full state access. Sec. IV addresses the output-feedback case, where identification and safe output regulation are achieved using only input-output data. The effectiveness of the proposed design is verified in Sec. V with a vehicle collision avoidance application. Finally, conclusions and future work are presented in Sec. VI.

F. Notation

- Define $\underline{x}_i(t) := (x_1(t), x_2(t), \dots, x_i(t))^\top$.
- The notation $L^2(0, 1)$ denotes the standard space of the equivalence class of square-integrable, measurable functions $u : \mathbb{R}^+ \times [0, 1] \rightarrow \mathbb{R}$, and $\|u(t)\| := (\int_0^1 u(x, t)^2 dx)^{\frac{1}{2}} < +\infty$ for $u \in L^2(0, 1)$. The norm $u[t]$ denote the profile of u at certain $t \geq 0$, i.e., $u[t] = u(x, t)$ for all $x \in [0, 1]$.
- The norm $|\cdot|$ denotes the usual Euclidean norm of the n -vector, $\|\cdot\|$ denotes the induced 2-norm of the matrix.
- The symbol \mathbb{R} denotes sets of real number and \mathbb{C} denotes sets of complex number, while \mathbb{N} denotes the set of all non-negative integers, \mathbb{N}^+ denotes all the natural numbers without 0, and $\mathbb{R}^+ := [0, \infty)$.
- The term I_n denote the $n \times n$ identity matrix and $\text{eig}(A)$ denotes all the eigenvalues of matrix A .
- The term $\text{sgn}(u)$ represents the signum function, i.e., $\text{sgn}(u) = \begin{cases} 1 & u > 0 \\ -1 & u \leq 0 \end{cases}$.

II. PROBLEM FORMULATION

A. Considered plant

Consider the uncertain strict-feedback linear system subject to the input delay and disturbances,

$$\dot{X}(t) = AX(t) + BU(t - D) + Gd(t), \quad (1)$$

$$Y(t) = CX(t), \quad (2)$$

where the states $X(t) = (x_1, \dots, x_n)^\top \in \mathbb{R}^n$, the unknown delay parameter $D \in \mathbb{R}$, the disturbance $d(t) \in \mathbb{R}^m$. To render the safe-regulation task more challenging, we consider the case with the highest relative degree. In this setting, the output matrix is $C = (1, 0, \dots, 0) \in \mathbb{R}^n$, so that the measured output is $Y(t) = x_1(t)$, i.e., the state farthest from the control input. Considering the structure of the strict-feedback systems, the form of the system matrix A and the input matrix are

$$A = \begin{pmatrix} a_{1,1} & 1 & & \\ a_{2,1} & a_{2,2} & 1 & \\ \vdots & \vdots & \ddots & \ddots \\ a_{n,1} & a_{n,2} & \dots & a_{n,n} \end{pmatrix}_{n \times n}, B = \begin{pmatrix} 0 \\ 0 \\ \vdots \\ b \end{pmatrix}_{n \times 1}. \quad (3)$$

All system parameters $b, a_{i,j}$ ($1 \leq i, j \leq n$) in (1) are unknown. The sign of the parameter b is known (without any loss of generality, $b > 0$ is given). In addition, we assume that (A, B) is controllable and (C, A) is observable.

Like [15], [29], the disturbances are supposed to be generated by the following finite-dimensional exogenous model

$$\dot{V}_d(t) = S_d V_d(t), \quad d(t) = P_d V_d(t), \quad (4)$$

where $V_d(t) = (v_{d,1}, \dots, v_{d,n_d})^\top \in \mathbb{R}^{n_d}$, and (P_d, S_d) is observable. The matrices $P_d \in \mathbb{R}^{m \times n_d}$ and $S_d \in \mathbb{R}^{n_d \times n_d}$ are unknown. The target trajectory $r(t) \in \mathbb{R}$ is considered to be generated by the exact known exogenous model

$$\dot{V}_r(t) = S_r V_r(t), \quad r(t) = P_r V_r(t), \quad (5)$$

where $V_r(t) = (v_{r,1}, \dots, v_{r,n_r})^\top \in \mathbb{R}^{n_r}$, (P_r, S_r) is observable. Thus, the dynamics of disturbance d and the reference r are unified by a finite-dimensional exogenous model

$$\dot{V}(t) = S V(t), \quad (6)$$

where $S = \text{diag}(S_d, S_r)$, $V(t) = \text{col}(V_d, V_r)$ and $n_v = n_d + n_r$. The matrix S is partially known, and all its eigenvalues are assumed to lie on the imaginary axis. It can generate constant or trigonometric signals that are common in practical applications. According to (4)–(6), d, r can be reformulated as

$$d(t) = \bar{P}_d V(t), \quad r(t) = \bar{P}_r V(t), \quad (7)$$

where $\bar{P}_d = (P_d, 0) \in \mathbb{R}^{m \times n_v}$, $\bar{P}_r = (0, P_r) \in \mathbb{R}^{1 \times n_v}$.

Model the delay D in (1) by the transport PDE, whose solution is

$$u(x, t) = \begin{cases} U(t - D + Dx), & \text{if } t - D + Dx > 0, \\ 0, & \text{if } t - D + Dx \leq 0 \end{cases} \quad (8)$$

for $x \in [0, 1]$, $t \in [0, \infty]$. Recalling (7), we have the equivalent representation of the original plant (1) as

$$\dot{X}(t) = AX(t) + Bu(0, t) + \bar{G}V(t), \quad (9)$$

$$Du_t(x, t) = u_x(x, t), \quad (10)$$

$$u(1, t) = U(t), \quad (11)$$

$$u(x, 0) = 0, \quad (12)$$

where $\bar{G} = G\bar{P}_d$ and $\bar{G} := (g_1; \dots; g_n) \in \mathbb{R}^{n \times n_v}$.

The unknown model parameters are:

$$\Theta = \underbrace{\{A, \bar{G}, S_d; D, b\}}_{\Theta_1} \quad (13)$$

It means that all plant parameters in the considered system are unknown except for S_d that is to generate the target trajectory and thus is known.

The following two assumptions about the bounds of unknown parameters in Θ_2 , are required in the control design, which are not restrictive because the bounds are arbitrary.

Assumption 1: The bound of the unknown delay parameter D is known and arbitrary, i.e., $D \in D_0$, where $D_0 := \{\mathcal{D} \in \mathbb{R} : 0 < \underline{D} \leq \mathcal{D} \leq \bar{D}\}$. The constants \underline{D}, \bar{D} are arbitrary and known.

Assumption 2: The bounds of the unknown parameter b is known and arbitrary, i.e., $b \in b_0$, where $b_0 := \{\beta \in \mathbb{R} : 0 < b \leq \beta \leq \bar{b}\}$. The constants \underline{b}, \bar{b} are arbitrary and known.

Considering the safety objectives, we further impose the following boundedness assumptions on all unknown parameters in Θ_1 :

Assumption 3: The bounds of unknown parameters in the system matrices A, S_d , and \bar{G} are known and arbitrary.

Assumption 3 means that the unknown parameters in Θ_1 belong to a known compact set $\bar{\Theta}_1$. It will be employed to derive a safe controller when the unknown parameters in Θ_1 have yet to be identified. However, if a control input that maintains the states within the safe region is known for a finite duration that exceeds the lower bound \underline{D} of delay, the assumption is no longer necessary.

B. Control objective

Define the output tracking error

$$e(t) = Y(t) - r(t) \quad (14)$$

and the safe set

$$\mathcal{C} = \{e(t) \in \mathbb{R} : h(e(t), t) \geq 0\}, \quad (15)$$

where $h(e(t), t)$ satisfies the following Assumption 4.

Assumption 4: The time-varying function h is n times differentiable with respect to each of its arguments, i.e., e as well as t , and satisfies that $\frac{\partial h(e, t)}{\partial e} \neq 0, \forall e \in \mathbb{R}, t \in [0, \infty]$. Besides, $|h(e(t), t)| < \infty \Rightarrow |e(t)| < \infty$ and $\lim_{t \rightarrow \infty} h(e(t), t) = 0 \Rightarrow e(t) = 0$.

The control objective is to design a controller to ensure the exponential convergence to zero of the error state $e(t)$, i.e.,

$$\lim_{t \rightarrow \infty} e(t) = Y(t) - r(t) = 0, \quad (16)$$

and keeping the error states $e(t)$ in the safe set \mathcal{C} , in the situation that almost all plant parameters are unknown.

III. CONTROL DESIGN WITH FULL STATE ACCESS

In this section, we first design a nominal safe controller using a three-step backstepping transformation, assuming full model knowledge. Then, addressing the scenario where nearly all plant parameters (13) are unknown, a data-driven approach that leverages the Koopman operator and Krylov DMD, along with a BaLSI identifier, is utilized to extract the underlying dynamics of the plant (1). Finally, we construct a safe controller that guarantees safety enforcement and exponential regulation, even in the presence of significant model uncertainties.

A. Nominal safe controller design

We proceed with the nominal control design following [48].

1) First transformation: Firstly, we introduce the linear coordinate transformation to incorporate the origin system (9) and the dynamics of the exogenous system (6) about disturbance and reference to convert into a vector chain of integrator:

$$Z(t) = T_z X(t) + T_v V(t), \quad (17)$$

where $Z(t) = (z_1, \dots, z_n)^\top$, and the matrices $T_z \in \mathbb{R}^{n \times n}$ as well as $T_v \in \mathbb{R}^{n \times n_v}$ are

$$T_z = \begin{pmatrix} 1 & & & & \\ \varrho_{2,1} & 1 & & & \\ \vdots & \ddots & \ddots & & \\ \varrho_{n,1} & \dots & \varrho_{n,n-1} & 1 \end{pmatrix} \quad (18)$$

, $T_v = -(\bar{P}_r; \sigma_1 + \bar{P}_r S^1; \dots; \sigma_{n-1} + \bar{P}_r S^{n-1})$. The constants $\varrho_{i,j}$ in T_z are defined as $\varrho_{1,1} = a_{1,1}, \varrho_{2,1} = a_{2,1} + \varrho_{1,1} a_{1,1}, \varrho_{2,2} = a_{2,2} + \varrho_{1,1}$, for $i = 3, \dots, n$, as $\varrho_{i,1} = a_{i,1} + \sum_{j=1}^{i-1} \varrho_{i-1,j} a_{j,1}, \varrho_{i,i} = a_{i,i} + \varrho_{i-1,i-1} + \sum_{j=i}^{i-1} \varrho_{i-1,j} a_{j,i}, \forall i = 2, \dots, i-1, \varrho_{i,i} = a_{i,i} + \varrho_{i-1,i-1}$, and the vectors σ_i are defined as $\sigma_0 = 0, \sigma_i = -\sum_{j=1}^{i-1} \varrho_{i-1,j} g_j - g_i + \sigma_{i-1} S, i = 1, \dots, n$. With this transformation, we obtain

$$\dot{Z}(t) = A_z Z(t) + B(u(0, t) + KX(t) + G_0 V(t)), \quad (19)$$

where

$$A_z = \begin{pmatrix} 0 & 1 & & & \\ & 0 & \ddots & & \\ & & \ddots & & \\ & & & 1 & \\ & & & & 0 \end{pmatrix}, K^\top = \frac{1}{b} \times \begin{pmatrix} \varrho_{n,1} \\ \vdots \\ \varrho_{n,n} \end{pmatrix}, \quad (20)$$

and $G_0 = -\frac{1}{b}(\sigma_n + \bar{P}_r S^n)$. Details of the transformation can be found in [48, Appendix 0.1]. To compensate for the delay, it is necessary to construct the prediction of system states. The prediction of $X(t)$ can be expressed as

$$X(t + \tau) = X(t) e^{A\tau} + \int_0^{\frac{\tau}{D}} D e^{DA(\frac{\tau}{D}-y)} B u(y, t) dy + \int_0^{\frac{\tau}{D}} D e^{DA(\frac{\tau}{D}-y)} \bar{G} e^{DSy} V(t) dy, \tau \in [0, D]. \quad (21)$$

2) Second transformations: Regarding the safe barrier function h , we introduce the second transformation

$$h_1(z_1(t), t) = h(e(t), t) + \varsigma(t), \quad (22)$$

$$h_i(z_i, t) = \sum_{j=1}^{i-1} \frac{\partial h_{i-1}}{\partial z_j} z_{j+1} + \frac{\partial h_{i-1}}{\partial t} + k_{i-1} h_{i-1}, \quad (23)$$

for $i = 2, \dots, n$. Like [48], $\varsigma(t)$ is introduced to handle the initially unsafe case. That is, if the error state $e(t)$ falls outside of the safe region at the initial regulation time $t = D$, i.e., $h(e(D), D) \leq 0$, the function $\varsigma(t)$ plays a role in rescuing to the defined safe region (15). The function $\varsigma(t)$ is given by

$$\varsigma(t) = \begin{cases} \begin{cases} (-h(e(D), D) + \epsilon) e^{\frac{1}{\bar{t}^2} - \frac{1}{(t-D-\bar{t})^2}}, & 0 \leq t < D + \bar{t} \\ 0, & t \geq D + \bar{t} \end{cases} \\ \begin{cases} if \quad h(e(D), D) \leq 0. \\ 0, \quad t \geq 0, \end{cases} \end{cases} \quad (24)$$

where ϵ is an arbitrarily positive design parameter, and the positive design parameter \bar{t} is the prescribed time for recovery to the safe region, which can be arbitrarily assigned by users. The value of $h(e(D), D)$ can be calculated at the initial time $t = 0$ by using $X(0), V(0)$, recalling (21), (1), (6). It is compactly written as

$$h(e(D), D) := \mathcal{P}_0(\chi(0), \Theta), \quad (25)$$

where

$$\chi(t) := (V(t), X(t)). \quad (26)$$

It is obtained from (24) that $\varsigma(t)$ is continuously differentiable of all orders. Therefore, together with Assumption 4, $h(e(t), t)$ is n times differentiable with respect to all its arguments $e(t)$ and t . Taking the partial derivative for $h(e(t), t)$ with respect to the variables $e(t)$, we have

$$\frac{\partial h(e(t), t)}{\partial e(t)} := \vartheta(e(t), t). \quad (27)$$

Given the linearity of the system, it follows from (22) and $e(t) = z_1(t)$ that $\frac{\partial h_n}{\partial z_n} = \frac{\partial h_{n-1}}{\partial z_{n-1}} = \frac{\partial h_{n-2}}{\partial z_{n-2}} = \dots = \frac{\partial h_1}{\partial z_1} = \frac{\partial h}{\partial e} = \vartheta$. Thus, applying the above transformations (22)–(24), defining $H = (h_1, \dots, h_n)^\top$, we have

$$\begin{aligned} \dot{H}(t) &= A_h H(t) + B \left(f(z_n(t), t) \right. \\ &\quad \left. + \vartheta(u(0, t) + KX(t) + G_0 V(t)) \right), \end{aligned} \quad (28)$$

where

$$A_h = \begin{pmatrix} -k_1 & 1 & & & \\ & -k_2 & \ddots & & \\ & & \ddots & & \\ & & & 1 & \\ & & & & -k_n \end{pmatrix}, \quad (29)$$

$$\text{and } f(z_n(t), t) = \frac{1}{b} \left(\sum_{j=1}^{n-1} \frac{\partial h_n}{\partial z_j} z_{j+1} + \frac{\partial h_n}{\partial t} + k_n h_n \right).$$

3) Third Transformation and controller: Now the intermediate system is (28) with u -PDE (10), (11). To remove the dependence on the signal model state and convert the intermediate system into an exponentially stable form, we introduce the following backstepping transformation:

$$\begin{aligned} w(x, t) &= u(x, t) - \int_0^x q(x, y) u(y, t) dy - \gamma(x) X(t) \\ &\quad - \bar{\gamma}(x) V(t) - \psi(x, t) \end{aligned} \quad (30)$$

where the solution of $q(x, y), \gamma(x), \psi(x, t)$, and that of the regulator equations $\bar{\gamma}(x)$, are given in Appendix A.

Applying (30), the intermediate system is (28), (10), (11) is converted into the target system

$$\dot{H}(t) = A_h H(t) + B \vartheta w(0, t), \quad (31)$$

$$Dw_t(x, t) = w_x(x, t) \quad (32)$$

$$w(1, t) = 0, \quad (33)$$

with choosing the nominal controller

$$\begin{aligned} U(t) &= - \int_0^1 D K e^{DA(1-y)} B u(y, t) dy - K e^{DA} X(t) \\ &\quad - \left(\int_0^1 D K e^{DAy} \bar{G} e^{DS(1-y)} dy + G_0 e^{DS} \right) V(t) + \psi(1, t) \\ &:= \mathcal{U}(\chi(t); \Theta), \end{aligned} \quad (34)$$

where

$$\begin{aligned}\psi(1, t) &= -\frac{f(z_n(t+D), t+D)}{\vartheta(z_1(t+D), t+D)} := \bar{\mathcal{P}}(Z(t), V(t), t, D) \\ &= \bar{\mathcal{P}}(T_z X(t) + T_v V(t), V(t), t, D),\end{aligned}\quad (35)$$

and where Θ defined in (13), and $\chi(t)$ defined in (26) are included in (34) to emphasize the controller's dependence on the signals $X(t)$, $V(t)$, and parameters Θ .

4) Selection of the design parameters: The selection of the gain parameters k_i in (23) is essential for both regulation and safety. These parameters are chosen to satisfy:

$$k_i \geq \max\{0, \hat{k}_i\}, i = 1, \dots, n-1, \quad k_n \geq 0, \quad (36)$$

where

$$\hat{k}_i(\chi(0); \Theta) = \frac{-1}{h_i(z_i(D), D)} \left(\sum_{j=1}^i \frac{\partial h_i}{\partial z_j} z_{j+1}(D) + \frac{\partial h_i}{\partial t} \right). \quad (37)$$

The vector $Z(D)$ can be precisely determined a priori at the initial time $t = 0$ by evaluating the state predictor (21).

5) Result of the nominal controller: We now present the following two lemmas to summarize the results achieved by the nominal controller.

Lemma 1: The high-relative-degree CBFs $h_i(t), i = 1, \dots, n$ are nonnegative under the selection of design parameters (36), (37), i.e., $h_i(t) \geq 0, i = 1, \dots, n$, for time $t \geq D$.

Proof: The proof is shown in Appendix B ■

Lemma 2: The tracking error $e(t)$ (14) in the closed-loop system (1), (2) with the nominal controller (34) converges to zero, and all system states remain bounded for any initial data $X(0) \in \mathbb{R}^n$, $V(0) \in \mathbb{R}^{n_v}$, and for any safety constraint $h(e, t)$ satisfying Assumption 4, provided that the design parameters k_1, \dots, k_n are chosen satisfying (36), (37).

Proof: The proof is shown in Appendix C ■

The aforementioned nominal controller $U(t)$ is built under the perfectly known plant model, while most parameters are considered unknown in this paper. The remainder of this section incorporates a data-driven design to identify the uncertainties from a finite-time collection of full-state data, and then construct a corresponding safe control based on the nominal controller design presented in (34).

B. Extract system dynamic Θ_1 using DMD

The presence of the input delay makes the plant behave as an autonomous system during the initial delay interval $t \in [0, D]$. This allows us to use DMD to extract important dynamic characteristics $\Theta_1 = \{A, \bar{G}, S_d\}$ without corruption from the external control input. We first introduce the piecewise constant function $\hat{\Theta}_1(t)$ to denote the estimated parameters of Θ_1 , and $\hat{\Theta}_1(0)$ is the arbitrary initial estimate of Θ_1 within the bounds in Assumptions 3.

1) The extended system with its Koopman operator: Recalling (1), (2), (4), during the initial period, the plant can be modeled as an autonomous extended system

$$\dot{\tilde{X}}(t) = \underbrace{\begin{pmatrix} S_d & 0 \\ GP_d & A \end{pmatrix}}_{\tilde{A}} \tilde{X}(t), \quad t \in [0, D] \quad (38)$$

where $\tilde{X}(t) = (V_d, X)^\top \in \mathbb{R}^{\tilde{n}}$ and $\tilde{n} = n + n_d$. Besides, the extended matrix $\tilde{A} \in \mathbb{R}^{\tilde{n} \times \tilde{n}}$ satisfies the following assumption:

Assumption 5: The eigenvalues of the matrix \tilde{A} are simple.

By stating that the eigenvalues are simple, we impose that the algebraic multiplicity of each eigenvalue is one such that the matrix \tilde{A} is diagonalizable. This assumption contributes to the clarity of the presentation. The proposed method can also be extended to the case of cyclic system matrices.

As shown in [17], the Koopman operator $\mathcal{K}(t)$ describes the evolution of the system (38) through observables $\phi(\tilde{X})$ according to $\mathcal{K}(t)\phi(\tilde{X}) = \phi(e^{\tilde{A}t}\tilde{X})$. Given the linearity of (38), the identity observable can be simply chosen as $\phi(\tilde{X}) = \tilde{X}$. The Koopman operator $\mathcal{K}(t)$ is characterized by its eigenfunctions $\tilde{\varphi}_i$ associated with eigenvalues $\tilde{\lambda}_i \in \mathbb{C}$. The Koopman eigenfunction $\tilde{\varphi}_i(\tilde{X})$ is an observable that evolves linearly in time, i.e., $\dot{\tilde{\varphi}}_i(\tilde{X}) = \tilde{\lambda}_i \tilde{\varphi}_i(\tilde{X})$, implying $\mathcal{K}(t)\tilde{\varphi}_i(\tilde{X}) = e^{\tilde{\lambda}_i t}\tilde{\varphi}_i(\tilde{X}), i = 1, \dots, \tilde{n}$. For the linear system (38), these eigenfunctions take the specific form [17]:

$$\tilde{\varphi}_i(\tilde{X}) = \langle \tilde{X}, \tilde{\omega}_i \rangle, \quad (39)$$

where $\langle \cdot, \cdot \rangle$ is the usual inner product and $\tilde{\omega}_i \in \mathbb{C}^{\tilde{n}}$ are the left eigenvectors of the system matrix \tilde{A} . Thus, the state \tilde{X} admits the spectral decomposition

$$\tilde{X} = \sum_{i=1}^{\tilde{n}} \tilde{\omega}_i \tilde{\varphi}_i(\tilde{X}) = \tilde{V} \tilde{\varphi}(\tilde{X}), \quad (40)$$

where $\tilde{V} = (\tilde{\omega}_1, \dots, \tilde{\omega}_{\tilde{n}}) \in \mathbb{C}^{\tilde{n}}$ is the matrix whose columns are the Koopman modes $\tilde{\omega}_i$ and $\tilde{\varphi}(\tilde{X}) = [\tilde{\varphi}_1(\tilde{X}), \dots, \tilde{\varphi}_{\tilde{n}}(\tilde{X})]$. Crucially, for the linear dynamics governed by \tilde{A} , these Koopman modes $\tilde{\omega}_i$ are the right eigenvectors of \tilde{A} , and the $\tilde{\lambda}_i$ are the corresponding eigenvalues. Especially, the Koopman modes for the observable \tilde{X} are calculated as

$$\tilde{\omega}_i = \begin{cases} (\nu_{d,i}, \nu_{x,i})^\top, & i = 1, \dots, n_d \\ (0, \nu_{x,i})^\top, & i = n_d + 1, \dots, \tilde{n} \end{cases} \quad (41)$$

where $S_d \nu_{d,i} = \tilde{\lambda}_i \nu_{d,i}$ with

$$\nu_{x,i} = (\tilde{\lambda}_i I - A)^{-1} G P_d \nu_{d,i} \quad (42)$$

for $i = 1, \dots, n_d$, and $A \nu_{x,i} = \tilde{\lambda}_i \nu_{x,i}$ for $i = n_d + 1, \dots, \tilde{n}$.

2) Krylov DMD: To identify the underlying dynamics Θ_1 of system (1) from state measurements, we collect data at discrete time intervals with a constant sampling period $T_d > 0$ satisfying the following assumption.

Assumption 6: The sampling time T_d satisfies $e^{\tilde{\lambda}_i T_d} \neq e^{\tilde{\lambda}_j T_d}, i \neq j, \forall \tilde{\lambda}_i, \tilde{\lambda}_j \in \text{eig}(\tilde{A}) \cup \text{eig}(S_d)$.

This assumption ensures that the observability and controllability of the continuous-time system are preserved when transitioning from the continuous-time domain to the sampled-data representation. Choosing a sampling period T_d based on Assumption 6 is straightforward, even though the matrices A and S_d are unknown. This is because the set of inadmissible sampling periods has a measure of zero, which renders the condition non-restrictive [17].

This process generates a sequence of data points, which are arranged into the data matrix:

$$\tilde{\mathcal{X}} = (\tilde{X}(0) \quad \tilde{X}(1) \quad \dots \quad \tilde{X}(2\tilde{n}-1)) \in \mathbb{R}^{\tilde{n} \times 2\tilde{n}}. \quad (43)$$

In this matrix, each column $\tilde{X}(k) = \tilde{X}(kT_d)$, $k \in \mathbb{N}$, is referred to as snapshots [40].

Remark 1: We are making use of the delay to identify the uncertainties. The uncertain D requires us to limit data collection in the interval $[0, \underline{D}]$, considering the known lower bound in Assumption 1. Consequently, the sampling time must satisfy $0 < T_d \leq \frac{\underline{D}}{2\tilde{n}-1}$. If \underline{D} is too small, the data collection period can be extended by applying zero input.

From the sequence of snapshots (43), we construct the Hankel matrix $H_{\tilde{n}}(\tilde{X})$:

$$H_{\tilde{n}}(\tilde{X}) = \begin{pmatrix} \tilde{X}(0) & \tilde{X}(1) & \dots & \tilde{X}(\tilde{n}-1) \\ \tilde{X}(1) & \tilde{X}(2) & \dots & \tilde{X}(\tilde{n}) \\ \vdots & \vdots & \vdots & \vdots \\ \tilde{X}(\tilde{n}-1) & \tilde{X}(\tilde{n}) & \dots & \tilde{X}(2\tilde{n}-2) \end{pmatrix} \in \mathbb{R}^{\tilde{n}^2 \times \tilde{n}}. \quad (44)$$

This matrix is known to admit the factorization

$$H_{\tilde{n}}(\tilde{X}) = Q_o Q_c, \quad (45)$$

where Q_o is the observability matrix and Q_c is the controllability matrix. They are defined as

$$Q_o = (I_{\tilde{n}} \quad \tilde{A}_d^\top \quad \dots \quad (\tilde{A}_d^{\tilde{n}-1})^\top)^\top \in \mathbb{R}^{\tilde{n}^2 \times \tilde{n}}, \quad (46)$$

$$Q_c = (\tilde{X}(0) \quad \tilde{A}_d \tilde{X}(0) \quad \dots \quad \tilde{A}_d^{\tilde{n}-1} \tilde{X}(0)) \in \mathbb{R}^{\tilde{n} \times \tilde{n}}. \quad (47)$$

where $I_{\tilde{n}}$ denotes the $\tilde{n} \times \tilde{n}$ identity matrix, and $\tilde{A}_d = e^{\tilde{A}T_d}$.

We now introduce several lemmas to describe the properties of the Hankel matrix $H_{\tilde{n}}(\tilde{X})$ and to show how system characteristics can be extracted from it.

Lemma 3: The Hankel matrix $H_{\tilde{n}}(\tilde{X})$ satisfies

$$\text{rank } H_{\tilde{n}}(\tilde{X}) = \tilde{n} \quad (48)$$

for almost all $\tilde{X}(0) \in \mathbb{R}^{\tilde{n}}$.

Proof: The proof is shown in Appendix D. \blacksquare

The full-rank property established in Lemma 3 enables the formulation of the Krylov DMD method [5], [17], [19], which we describe as follows.

Lemma 4: If $H_{\tilde{n}}(\tilde{X}) = \tilde{n}$,

$$\mathcal{K}(T_d) H_{\tilde{n}}(\tilde{X}) = H_{\tilde{n}}(\tilde{X}) \underbrace{\begin{pmatrix} 0 & 0 & \dots & 0 & -f_0 \\ 1 & 0 & \dots & 0 & -f_1 \\ 0 & 1 & \dots & 0 & -f_2 \\ \vdots & \vdots & \ddots & 0 & \vdots \\ 0 & 0 & \dots & 1 & -f_{\tilde{n}-1} \end{pmatrix}}_{F \in \mathbb{R}^{\tilde{n} \times \tilde{n}}} \quad (49)$$

with

$$\begin{aligned} f &= \text{col}(f_0, \dots, f_{\tilde{n}-1}) \\ &= -(H_{\tilde{n}}^\top(\tilde{X}) H_{\tilde{n}}(\tilde{X}))^{-1} H_{\tilde{n}}^\top(\tilde{X}) \text{col}(\tilde{X}(\tilde{n}), \dots, \tilde{X}(2\tilde{n}-1)) \end{aligned} \quad (50)$$

holds.

Proof: Its proof can be found in [17, Lemma 3]. \blacksquare

The next step is crucial, which derives the Koopman modes, eigenvalues, and eigenfunctions from the companion matrix F .

Lemma 5: If $H_{\tilde{n}}(\tilde{X}) = \tilde{n}$, and letting $\hat{\nu}_i, i = 1, \dots, \tilde{n}$ be the eigenvectors of F coinciding with the corresponding

eigenvalues $\hat{\lambda}_i$, the Koopman eigenvalues can be computed from

$$\tilde{\lambda}_i = \frac{\ln \hat{\lambda}_i}{T_d}, \quad i = 1, \dots, \tilde{n} \quad (51)$$

including the eigenvalues $\tilde{\lambda}_i, i = 1, \dots, n_d$, of the disturbance model S_d in (4) and $\tilde{\lambda}_i, i = n_d + 1, \dots, \tilde{n}$ of the system matrix A in (1). The Koopman modes $\tilde{\nu}_i$ corresponding of the Koopman eigenvalues $\tilde{\lambda}_i$ is

$$\tilde{\nu}_i = [I_{\tilde{n}} \quad 0] H_{\tilde{n}}(\tilde{X}) \hat{\nu}_i, \quad i = 1, \dots, \tilde{n}. \quad (52)$$

Proof: The proof is shown in Appendix E. \blacksquare

Lemma 6: If $\text{rank } H_{\tilde{n}}(\tilde{X}) = \tilde{n}$, the exact identification of the unknown system dynamics Θ_1 is achieved at $t = \underline{D}$, that is $\hat{\Theta}_1(\underline{D}) = \{\mathcal{A}, S_d, \bar{\mathcal{G}}\} = \Theta_1$, where

$$\mathcal{A} = (\mathbf{0} \quad I_n) \tilde{\mathcal{A}} (\mathbf{0} \quad I_n)^\top, \quad (53)$$

$$S_d = (I_{n_d} \quad \mathbf{0}) \tilde{\mathcal{A}} (I_{n_d} \quad \mathbf{0})^\top, \quad (54)$$

$$\bar{\mathcal{G}} = \left((\mathbf{0} \quad I_n) \tilde{\mathcal{A}} (I_{n_d} \quad \mathbf{0})^\top \quad \mathbf{0} \right), \quad (55)$$

with identifying $\tilde{\mathcal{A}}$ by

$$\tilde{\mathcal{A}} = \tilde{V} \tilde{\Lambda} \tilde{V}^{-1}. \quad (56)$$

The matrices \tilde{V} and $\tilde{\Lambda} = \text{diag}(\tilde{\lambda}_1, \dots, \tilde{\lambda}_n)$ obtained from Lemma 5.

Proof: The proof is shown in Appendix F. \blacksquare

C. Identification of parameters Θ_2

Following [46], we use a batch of actuation and plant data collected over a duration to build the following identifier:

$$\begin{aligned} \hat{\Theta}_2(t_{i+1}) &= \arg \min \left\{ |\ell - \hat{\Theta}_2(t_i)|^2 : \ell \in \bar{\Theta}_2, \right. \\ &\quad \left. \bar{F}_n(t_{i+1}, \mu_{i+1}) = \bar{Q}_n(t_{i+1}, \mu_{i+1})\ell, n = 1, 2, \dots \right\}, \end{aligned} \quad (57)$$

to estimate the unknown parameters $\Theta_2 = \{D, b\}$, i.e., the unknown delay and the parameter in the input matrix B , where $\hat{\Theta}_2(t_i) = (\hat{D}(t_i), \hat{b}(t_i))$ and the set

$$\bar{\Theta}_2 := \{\ell \in \mathbb{R}^2 : \underline{D} \leq \ell_D \leq \bar{D}, b \leq \ell_b \leq \bar{b}\} \quad (58)$$

uses the known bounds given in Assumption 1, 2. The parameter estimates (57) are updated at the discrete sequence of time instants $\{t_i \geq 0\}_{i=0}^\infty, i = 0, 1, 2, \dots$, by employing the fixed-time triggering mechanism: $t_{i+1} = t_i + T_a$, where $T_a > 0$ is a design parameter satisfying $t_1 = t_0 + T_a \geq \underline{D}$. Above condition ensures that updates commence only after the DMD identification of $a_{n,i}$ completes at $t = \underline{D}$, as these parameters are required to compute (57) (specifically $f_b(t)$).

Each new estimate at t_{i+1} is computed using a batch of historical plant data collected over the time window $[\mu_{i+1}, t_{i+1}]$. The start of this window μ_{i+1} is defined as:

$$\mu_{i+1} := \min\{t_g : g \in 0, \dots, i, t_g \geq t_{i+1} - \tilde{N}T\}, \quad (59)$$

where $\tilde{N} \geq 1$ is a free integer parameter. The matrices \bar{F}_n and \bar{Q}_n used in the estimator (57) are defined as: $\bar{F}_n = (F_n, F_b)^\top$,

$\bar{Q}_n = \begin{pmatrix} Q_n & 0 \\ 0 & Q_b \end{pmatrix}$. Their components are computed by integrating signals over the data window $[\mu_{i+1}, t_{i+1}]$:

$$F_n = \int_{\mu_{i+1}}^{t_{i+1}} f_n(t) q_n(t) dt, \quad Q_n = \int_{\mu_{i+1}}^{t_{i+1}} q_n(t)^2 dt, \quad (60)$$

$$F_b = \int_{\mu_{i+1}}^{t_{i+1}} f_b(t) q_b(t) dt, \quad Q_b = \int_{\mu_{i+1}}^{t_{i+1}} q_b(t)^2 dt,$$

where $q_n(t) = -\int_0^1 \sin(x\pi n) u(x, t) dx$, $f_n(t) = \pi n \int_0^t \int_0^1 \cos(x\pi n) u(x, \tau) dx d\tau$, $f_b(t) = x_n(t) - x_n(0) - \int_0^t \sum_{i=1}^n a_{n,i} x_i(\tau) d\tau - \int_0^t g_n V(\tau) d\tau$, $q_b(t) = \int_0^t u(0, \tau) d\tau$.

We briefly describe the design procedure of (57) below. It is obtained from (9)–(12) that $f_n(t) = D q_n(t)$, $f_b(t) = b q_b(t)$, based on which the quadratic function $\Xi_{i,n} : \mathbb{R}^2 \rightarrow \mathbb{R}_+$ is constructed as $\Xi_{i,n}(\ell) = \int_{\mu_{i+1}}^{t_{i+1}} [(f_n - \ell_D q_n)^2 + (f_b - \ell_b q_b)^2] dt$, for $i \in \mathbb{N}$, where $\ell = (\ell_D, \ell_b)^\top$. It follows that the true parameter vector Θ_2 is the unique global minimum, such that the gradient of $\Xi_{i,n}(\ell)$ vanishes here according to Fermat's theorem. Thus, taking the partial derivatives to $\Xi_{i,n}$ with respect to ℓ_D, ℓ_b to zero yields that $\bar{F}_n(t_{i+1}, \mu_{i+1}) = \bar{Q}_n(t_{i+1}, \mu_{i+1}) \Theta_2$ for each mode $n \in \mathbb{N}$ and update step $i \in \mathbb{N}$. The estimator (57) is then derived from such a batch least-squares solution. More details can be found in [47].

Lemma 7: The finite-time exact identification of the unknown parameters Θ_2 is achieved, that is, there exists a finite time t_f defined by

$$t_f = \min\{t_i : \exists t \in [0, t_i], u(0, t) \neq 0\}, \quad (61)$$

such that $\hat{\Theta}_2(t_f) \equiv \Theta_2, \forall t \geq t_f$.

Proof: Its proof is very similar to the proofs of Lemma 4 in [47] and Sec. IV-C of [46]. Due to space constraints, they are omitted here. \blacksquare

D. Data-Driven Safe Control

In this section, we build a data-driven safe controller by combining the nominal design in Sec. III-A and the data-driven identification process in Secs. III-B, III-C. Replacing the unknown parameters by their real-time estimates $\hat{\Theta}(t) = (\hat{\Theta}_1(t), \hat{\Theta}_2(t))$ in the nominal safe control law (34), we have

$$U_d(t) := \mathcal{U}(\chi(t); \hat{\Theta}(t)), \quad (62)$$

where $\hat{\Theta}(t)$ is piecewise-constant vector recalling the designs in Secs. III-B, III-C:

$$\hat{\Theta}(t) = \begin{cases} (\hat{\Theta}_1(0), \hat{\Theta}_2(0)), & t \in [0, \underline{D}] \\ (\hat{\Theta}_1(\underline{D}), \hat{\Theta}_2(0)), & t \in [\underline{D}, t_f] \\ (\hat{\Theta}_1(\underline{D}), \hat{\Theta}_2(t_f)), & t \in [t_f, \infty) \end{cases} \quad (63)$$

where $\hat{\Theta}_1(0), \hat{\Theta}_2(0)$ are the initial estimates, and $\hat{\Theta}_1(\underline{D}) = \{\mathcal{A}, \mathcal{S}_d, \mathcal{G}\}$, which are obtained by (53), is the exact identification of Θ_1 according to Lemma 6, and $\hat{\Theta}_2(t_f)$ is the exact identification of Θ_2 according to Lemma 7.

Different from the nominal control U , here $U_d(t)$ is potentially unsafe due to the identification error of Θ for $t \in [0, t_f]$. Especially, the safety mechanism designed about (24), (37) relies on the exact value of $h(e(D), D)$ recalling (25), which is inaccessible in the case of the uncertain plant. We instead compute its lower and upper bounds, \underline{h} and \bar{h} , over the

parameter uncertainty sets $\bar{\Theta}_1, \bar{\Theta}_2$ defined in Assumptions 3 and (58), as $\bar{h} = \max_{\theta_1 \in \bar{\Theta}_1, \theta_2 \in \bar{\Theta}_2} \mathcal{P}_0(\chi(0); \theta_1, \theta_2)$,

$$\underline{h} = \min_{\theta_1 \in \bar{\Theta}_1, \theta_2 \in \bar{\Theta}_2} \mathcal{P}_0(\chi(0); \theta_1, \theta_2), \quad (64)$$

For (24), the sign of $h(e(D), D)$ should be known. Therefore, we impose the following assumption to ensure the sign is unambiguous:

Assumption 7: The lower and upper bounds \underline{h} and \bar{h} have the same sign, i.e., they satisfy either $\bar{h} \leq 0$ or $\underline{h} \geq 0$.

This assumption ensures that the interval $[\underline{h}, \bar{h}]$ does not contain zero, which allows the sign of $h(e(D), D)$ to be determined a priori despite parametric uncertainties by evaluating the bounds \underline{h}, \bar{h} . When Assumption 4 does not hold, the sign of $h(e(D), \bar{D})$ cannot be reliably inferred in the presence of uncertainties. Therefore, the system has to be conservatively treated as unsafe at that instant, i.e., $h(e(D), D) \leq 0$ is adopted in the subsequent control design, which will lead to rigorous safety guarantees established starting from $t = \bar{D} + \bar{t}$ with a positive \bar{t} assigned by users.

Then the modified function ς (24) is introduced as

$$\varsigma(t) = \begin{cases} (-\underline{h} + \epsilon) e^{\frac{1}{\bar{t}^2} - \frac{1}{(t - \bar{D} - \bar{t})^2}}, & 0 \leq t < \bar{D} + \bar{t}, \\ 0, & t \geq \bar{D} + \bar{t} \\ \quad \text{if } \bar{h} \leq 0. \\ 0, & t \geq 0, \quad \text{if } \underline{h} > 0 \end{cases} \quad (65)$$

where the positive design parameters ϵ and \bar{t} are free. The role of (65) is to drive the state that is unsafe initially to the safe region by a prescribed time $\bar{D} + \bar{t}$.

Also, the selection of the design parameter k_i is modified to account for model uncertainty by using the known parameter bounds from Assumptions 1–3:

$$k_i \geq \max_{\theta_1 \in \bar{\Theta}_1, \theta_2 \in \bar{\Theta}_2} \{0, \hat{k}_i(\chi(0); \theta_1, \theta_2)\}, i = 1, \dots, n-1 \quad (66)$$

and $k_n \geq 0$, where \hat{k}_i is obtained from substituting the variable θ_1, θ_2 for the unknown Θ in (37), which are specified by the bounds in Assumptions 3 and (58), respectively. This choice guarantees the initial positivity of $h_i(z_i(D), D)$, $i = 2, \dots, n$ from $h_1(z_1(D), D) > 0$ ensured by (65).

To ensure robust safety against all possible parameter values before identification is complete, we construct the following safe controller under uncertainty:

$$U_a(t) = \begin{cases} \frac{1}{\vartheta_0} \max_{\theta_1 \in \bar{\Theta}_1, \theta_2 \in \bar{\Theta}_2} \vartheta_0 \mathcal{U}(\chi(t); \theta_1, \theta_2), & 0 \leq t < \underline{D} \\ \frac{1}{\vartheta_0} \max_{\theta_2 \in \bar{\Theta}_2} \vartheta_0 \mathcal{U}(\chi(t); \hat{\Theta}_1(\underline{D}), \theta_2), & \underline{D} \leq t < t_f, \\ U_d(t), & t \geq t_f \end{cases} \quad (67)$$

where

$$\vartheta_0 := \text{sgn}(\vartheta(e(0), 0)). \quad (68)$$

The switching time t_f is the triggering time when the exact parameter identification is achieved, determined by (61). The diagram of the closed-loop system about the proposed data-driven safe control is depicted in Fig.1, and the result is presented in the next subsection.

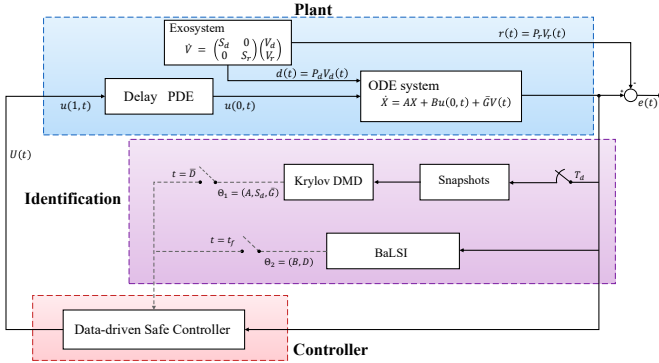


Fig. 1: Diagram of the proposed data-driven safe control system.

E. Result with the controller under uncertainty

Definition 1: The initial safety condition is defined as: the safety is ensured in the uncontrolled period $t \in [0, D]$, i.e., $h(e(t), t) \geq 0, \forall t \in [0, D]$ and $h(e(D), D) \neq 0$. It means that the safety holds for the uncontrolled period at the beginning and the error state $e(t)$ does not stay at the safe boundary at the initial regulation time $t = D$.

Theorem 1: For initial data $X(0) \in \mathbb{R}^n$, $V(0) \in \mathbb{R}^{n_v}$, and the safety constraint $h(e, t)$ satisfying Assumptions 4, 7, choosing the design parameters k_1, \dots, k_n satisfying (66), the closed-loop system consisting of the disturbed linear plant (1), (2) with unknown Θ (13), and the data-driven safe controller (67), has the following properties

- 1) There exists a unique solution $X(t) \in \mathbb{R}^n$, $V(t) \in \mathbb{R}^{n_v}$, $u[t] \in L^2(0, 1)$ to the system (9)–(12) with control input (67).
- 2) The identification $\hat{\Theta}(t)$ of unknown parameters Θ is bounded and reaches the true value in finite time t_f that is defined in (61).
- 3) Tracking error state $e(t)$ (14) is convergent to zero and all states are bounded;
- 4) The safety is ensured in the sense that
 - a) If the initial safe condition in Definition 1 is met, then safety is guaranteed for $t \in [0, \infty)$.
 - b) If the initial safe condition in Definition 1 is not met, but $h(e(D), D) > 0$, then safety is guaranteed for $t \geq D$.
 - c) If the initial safe condition in Definition 1 is not met, and $h(e(D), D) \leq 0$, the safety is guaranteed for $t \geq D + \bar{t}$ where $\bar{t} > 0$ can be arbitrarily assigned by users.

Proof: 1) From the initial condition (8) and the transformations (17), (22), (23), as well as the exogenous signal model (6), we have $w[0] \in L^2(0, 1)$, $H(0) \in \mathbb{R}^n$, and $V(t) \in \mathbb{R}^{n_v}$. Defining the difference between U_a (67) and the nominal controller (34) as $\eta(t) = U_a(t) - U(t)$. and applying the designed controller $U_a(t)$ to the plant (9)–(12), the target system becomes (31), (32) with

$$w(1, t) = \eta(t). \quad (69)$$

We know that the difference $\eta(t)$ originates from the parameter mismatch error and only contains system signals $\chi(t)$ defined in (26). Thus, by defining the norm as $\Omega(t) = |X(t)|^2 + |V(t)|^2 + \|u(t)\|^2$ and applying the transformations (17), (22),

(23) along with the predictions (21), we can establish the following inequality for some positive constant \mathcal{N} : $\eta^2(t) \leq \mathcal{N}\Omega(t)$. The inherent boundedness of the linear system with bounded input over a finite horizon ensures that the norm $\Omega(t)$ is bounded. From the above inequality, it directly follows that $\eta(t)$ is bounded within $t \in [0, t_f]$. The controller switching in (67) ensures that $\eta(t)$ is zero for $t \geq t_f$. Then, we obtain that $w[t] \in L^2(0, 1)$ with $w[0] \in L^2(0, 1)$ from (69), (32). Recalling the target system (31), (32), (69), we have the solution of ODE that $H(t) = H(0)e^{A_h t} + \int_0^t e^{A_h(t-\tau)} B\vartheta(e(\tau), \tau)w(0, \tau) d\tau$. Together with the boundedness of $w[t]$ and boundedness of ϑ (27) from Assumption 4, it follows that $H(t)$ on $t \in [0, \infty)$ is bounded. Following the recursive process in the proof of Lemma 2 shown in Appendix C, we know that all $\frac{\partial h_i}{\partial z_j}, 1 \leq j \leq i \leq n, i, j \in \mathbb{N}$ are bounded. It further concludes that $Z(t) \in \mathbb{R}^n$ considering $H(t) \in \mathbb{R}^n$ and (22)–(24). Then, $X(t) \in \mathbb{R}^n$ is obtained from (17). Applying the Cauchy-Schwarz inequality to the inverse transformation (A.4), we have that $u[t] \in L^2(0, 1)$ is then obtained from $w[t] \in L^2(0, 1)$. The proof of this property is complete.

2) According to Lemmas 6, 7, we directly obtain the property 2) that the parameter identification $\hat{\Theta}(t)$ achieves the true value Θ in finite time t_f .

3) In the target system (31), (32) with (69), the difference η in (69) will vanish after a finite time $t = t_f$, recalling Property 2) and (69). Together with that the matrix A_h in (28) is Hurwitz, $|H(t)|$ is thus exponentially convergent to zero. Then, follow the same process in proving Lemma 2 in Appendix C, this property is obtained.

4) For the target system (31), (32) with (69), the sign of $\vartheta(t)$ defined in (27), is constant, because Assumption 4 implies that the function $\vartheta(e(t), t)$ is continuous and nonzero. As a result, $\text{sgn}(\vartheta(t))$ is equal to ϑ_0 defined in (68). Considering (69) and (32), it is known that $b\vartheta w(0, t) \geq 0$ for all $t \in [D, t_f + D]$. Recalling (66), the positivity of the initial barrier function value, i.e., $h_i(z_i(D), D)$, is guaranteed by design parameters k_i which belong to the subset of (36). Therefore, from the structure of $H(t)$ in (31), we know that all barrier functions h_i are nonnegative during the time period $t \in [D, \infty)$, i.e., $h_i(t) \geq 0$ is ensured for all $t \geq D$. Next, we prove property 3) about safety by examining each of the three cases:

a) Because the initial safe condition in Definition 1 is met, (65) directly imply $\varsigma(t) \equiv 0$. Consequently, by (22), $h(e(t), t) = h_1(z_1(t), t) \geq 0$ for all $t \geq D$. Together with the initial condition, this establishes system safety, $h(e(t), t) \geq 0$, for all time $t \in [0, \infty)$.

b) Even though the safety is not guaranteed during the period $[0, D]$ in this case, considering $h(e(D), D) \geq 0$ and through the same process with the proof in a), we have $h(e(t), t) \geq 0$ holds on $t \in [D, \infty)$.

c) We know that $\varsigma(t)$ is identically zero after a preset finite time $t \geq D + \bar{t}$ according to (65). It follows (22) that $h(e(t), t) = h_1(z_1(t), t) \geq 0$ for all $t \geq D + \bar{t}$. Thus, safety is guaranteed after a finite time $t \geq D + \bar{t}$.

The proof of this theorem is complete. \blacksquare

IV. CONTROL DESIGN USING OUTPUT DATA

In contrast to the preceding full-state feedback design, this section addresses a more practical situation in which only the output state is measurable. We develop an output-feedback safe controller by reconstructing the system and disturbance dynamics directly from output measurements.

Given the very limited amount of data available for identification, in addition to Assumptions 1, 3, it is necessary to impose the following additional assumptions. For the original plant (1), (2), and the exogenous model (4)–(6), we now assume that the matrices B, G, P_d , which characterize the channels through which the control input and external disturbances act on the system, are known. The system matrices A, S_d of the plant and disturbances remain unknown, but are assumed to take the following companion form:

$$A = \begin{pmatrix} 0 & 1 & & \\ & \ddots & \ddots & \\ & & 0 & 1 \\ a_1 & \dots & a_{n-1} & a_n \end{pmatrix}, S_d = \begin{pmatrix} 0 & 1 & & \\ & \ddots & \ddots & \\ & & 0 & 1 \\ \beta_1 & \dots & \beta_{n_d-1} & \beta_{n_d} \end{pmatrix}. \quad (70)$$

Accordingly, the unknown argument Θ (13) becomes

$$\Theta = \underbrace{\{A, S_d, D\}}_{\Theta_1}. \quad (71)$$

Additionally, the following assumption ensures the unknown initial states are within a known compact set $\bar{\zeta}_0$, which is required for ensuring safety before the plant states and disturbances are successfully estimated by the data-driven observer.

Assumption 8: The bounds of the initial states $X(0)$ of the plant and the initial values $V_d(0)$ of the exogenous signal are known and arbitrary.

The safe barrier function h satisfies Assumptions 4, 7. Besides, given that the system state and disturbances are unmeasured in this section, we impose an additional assumption for the barrier function h :

Assumption 9: The barrier function h ensures that there exists a positive ξ_e such that

$$\tilde{\mathcal{P}}(\tilde{V}(t), \tilde{X}(t)) \leq \xi_e(|\tilde{V}(t)| + |\tilde{X}(t)|) \quad (72)$$

where $\tilde{\mathcal{P}} := \bar{\mathcal{P}}(T_z X(t) + T_v V(t), V(t), t) - \bar{\mathcal{P}}(T_z \hat{X}(t) + T_v \hat{V}(t), \hat{V}(t), t)$ and $\bar{\mathcal{P}}$ (35) is determined by (22)–(27).

A. Identification of the unknown system dynamics

In this section, we identify system parameters only from input-output data to construct an extended observer for unmeasured states and disturbances, a prerequisite for safe output regulation. During the period $t \in [0, \underline{D}]$, we introduce the extended system (38) as well. Following the methodology of Sec. III-B, we apply the Koopman operator $\mathcal{K}(t)$ to the observable \tilde{X} (40), employing the same set of Koopman elements: the eigenfunction $\tilde{\varphi}(\tilde{X})$ (39), modes $\tilde{\nu}_i$ (41), and eigenvalues $\tilde{\lambda}_i$. As with (43), data is collected at a fixed sampling time T_d over the interval, consistent with Assumption 6 and Remark 1. Accordingly, the measurement data matrix is constructed exclusively from the output signals $Y(t)$ (2):

$$\tilde{\mathcal{Y}} = (Y(0) \quad Y(1) \quad \dots \quad Y(2\tilde{n}-1)) \in \mathbb{R}^{1 \times 2\tilde{n}} \quad (73)$$

with snapshots $Y(k) = Y(kT_d), k \in \mathbb{N}$.

Accordingly, the output is expressed using the extended state \tilde{X} as $Y = \bar{C}\tilde{X}$, where $\bar{C} = (0 \quad C)$. From the output data sequence in (73), we form the Hankel matrix

$$H_{\tilde{n}}(Y) = \begin{pmatrix} Y(0) & Y(1) & \dots & Y(\tilde{n}-1) \\ Y(1) & Y(2) & \dots & Y(\tilde{n}) \\ \vdots & \vdots & \vdots & \vdots \\ Y(\tilde{n}-1) & Y(\tilde{n}) & \dots & Y(2\tilde{n}-2) \end{pmatrix} \in \mathbb{R}^{\tilde{n} \times \tilde{n}}. \quad (74)$$

This Hankel matrix can also be factorized into the product of the extended observability and controllability matrices, i.e., $H_{\tilde{n}}(Y) = Q_o Q_c$, where Q_c is given by (47) and Q_o is the extended observability matrix

$$Q_o = (\bar{C}^\top \quad (\bar{C}\tilde{A}_d)^\top \quad \dots \quad (\bar{C}\tilde{A}_d^{\tilde{n}-1})^\top)^\top \in \mathbb{R}^{\tilde{n} \times \tilde{n}}. \quad (75)$$

Unlike [17], which requires the output dimension to be no less than the disturbance dimension, the following lemma establishes a full-rank condition for $H_{\tilde{n}}(Y)$ using only low-dimensional output data.

Lemma 8: If

$$\text{rank} \begin{pmatrix} A - \tilde{\lambda}I & GP_d \\ C & 0 \end{pmatrix} = n+1, \quad \forall \tilde{\lambda} \in \text{eig}(S_d), \quad (76)$$

the Hankel matrix $H_{\tilde{n}}(Y)$ satisfies

$$\text{rank } H_{\tilde{n}}(Y) = \tilde{n} \quad (77)$$

for almost all $Y(0) \in \mathbb{R}$.

Proof: The proof is shown in Appendix G. \blacksquare

Given that the Hankel matrix $H_{\tilde{n}}(Y)$ has full rank, as established in Lemma 8, it is natural to apply the Krylov DMD method to extract the system's dynamic characteristics, as follows.

Lemma 9: If $\text{rank } H_{\tilde{n}}(Y) = \tilde{n}$,

$$\mathcal{K}(T_d)H_{\tilde{n}}(Y) = H_{\tilde{n}}(Y) \underbrace{\begin{pmatrix} 0 & & -f_0 \\ 1 & 0 & -f_1 \\ \ddots & \ddots & \vdots \\ 1 & -f_{\tilde{n}-1} \end{pmatrix}}_{F \in \mathbb{R}^{\tilde{n} \times \tilde{n}}} \quad (78)$$

with

$$\begin{aligned} f &= \text{col}(f_0, \dots, f_{\tilde{n}-1}) \\ &= -(H_{\tilde{n}}^\top(Y)H_{\tilde{n}}(Y))^{-1}H_{\tilde{n}}^\top(Y)\text{col}(Y(\tilde{n}), \dots, Y(2\tilde{n}-1)) \end{aligned} \quad (79)$$

holds.

Proof: Its proof can be found in [17, Lemma 3]. \blacksquare

Next, we extract the Koopman eigenvalues from matrix F (78), and subsequently identify the system dynamic matrix.

Lemma 10: Assume that $\text{rank } H_{\tilde{n}}(Y) = \tilde{n}$, and let $\hat{\nu}_i, i = 1, \dots, \tilde{n}$ be the eigenvectors of F coincide with the corresponding eigenvalues $\hat{\lambda}_i$. The Koopman eigenvalues can be computed from

$$\tilde{\lambda}_i = \frac{\ln \hat{\lambda}_i}{T_d}, \quad i = 1, \dots, \tilde{n} \quad (80)$$

including the eigenvalues $\tilde{\lambda}_i, i = 1, \dots, n_d$, of the disturbance model S_d in (70) and $\tilde{\lambda}_i, i = n_d + 1, \dots, \tilde{n}$ of the system

matrix A in (70). The exact identification of the unknown system dynamics $\Theta_1 = \{A, S_d\}$ is achieved at $t = \underline{D}$, that is $\hat{\Theta}_1(\underline{D}) = \{\mathcal{A}, \mathcal{S}_d\} \equiv \Theta_1$, where

$$\mathcal{A} = V_A \Lambda_A V_A^{-1}, \quad \mathcal{S}_d = V_d \Lambda_d V_d^{-1}, \quad (81)$$

with $\Lambda_A = \text{diag}(\tilde{\lambda}_{n_d+1}, \dots, \tilde{\lambda}_{\tilde{n}})$, $\Lambda_d = \text{diag}(\tilde{\lambda}_1, \dots, \tilde{\lambda}_{n_d})$, and the eigenvector matrices

$$V_A = \begin{pmatrix} 1 & \dots & 1 \\ \tilde{\lambda}_{n_d+1} & \dots & \tilde{\lambda}_{\tilde{n}} \\ \vdots & \ddots & \vdots \\ \tilde{\lambda}_{n_d+1}^{n-1} & \dots & \tilde{\lambda}_{\tilde{n}}^{n-1} \end{pmatrix}, \quad V_d = \begin{pmatrix} 1 & \dots & 1 \\ \tilde{\lambda}_1 & \dots & \tilde{\lambda}_{n_d} \\ \vdots & \ddots & \vdots \\ \tilde{\lambda}_1^{n_d-1} & \dots & \tilde{\lambda}_{n_d}^{n_d-1} \end{pmatrix}, \quad (82)$$

as Vandermonde matrices constructed from the corresponding eigenvalues.

Proof: The proof is shown in Appendix H. \blacksquare

In addition to (81), alternatively, the coefficients a_i, d_i in the matrices A, S_d (70) can be obtained by the coefficients of the characteristic polynomial using all known eigenvalues $\tilde{\lambda}_i$.

To estimate the unknown delay parameter D , we adapt the same BALSI design in Sec. III-C to build the delay identifier. Since only D is unknown, the general parameter estimator (57) simplifies to

$$\hat{D}(t_{i+1}) = \arg \min \left\{ |\ell - \hat{D}(t_i)|^2 : \ell \in D_0, F_n(t_{i+1}, \mu_{i+1}) = Q_n(t_{i+1}, \mu_{i+1})\ell, n = 1, 2, \dots \right\}, \quad (83)$$

where F_n, Q_n are defined as in (60), and the set $D_0 := \{\ell \in \mathbb{R} : \underline{D} \leq \ell \leq \bar{D}\}$ is given in Assumption 1.

Lemma 11: The finite-time exact identification of the unknown parameters D is achieved, that is, there exists a finite time t_f defined by

$$t_f = \min \{t_i : \exists t \in [0, t_i], u[t] \neq 0\}, \quad (84)$$

such that $\hat{D}(t_f) = \mathcal{D} \equiv D, \forall t \geq t_f$.

Proof: Its proof can be found in Sec. IV-C of [46]. \blacksquare

B. Design of observer under uncertain dynamics

Based on the data-driven parameter identification provided in the last subsection, we establish an extended state observer for the unmeasured states and disturbances of the system (9)–(12), relying on the output data $Y(t)$ in (2). Treating the disturbances as extended states, the state observer for the extended system consisting of (1), (2) (4) is designed as

$$\begin{aligned} \dot{\hat{X}}(t) &= \hat{A}(t)\hat{X}(t) + BU(t - \hat{D}(t)) + GP_d\hat{V}_d(t) \\ &\quad + L_x(t)(Y(t) - \hat{Y}(t)), \end{aligned} \quad (85)$$

$$\dot{\hat{V}}_d(t) = \hat{S}_d(t)\hat{V}_d(t) + L_v(t)(Y(t) - \hat{Y}(t)), \quad (86)$$

$$\hat{Y}(t) = C\hat{X}(t), \quad (87)$$

where \hat{X} is the estimate of the state vector X , $\hat{V}_d(t)$ is the estimate of the unmeasured disturbance $V_d(t)$, and the observer gains, $L_v(t)$ and $L_x(t)$ are designed later. The system matrices used in the observer are the identified values of A and S_d , denoted as $\hat{A}(t)$ and $\hat{S}_d(t)$. Specifically, as established in Lemma 10, these estimates are piecewise constant and

converge in finite time: $\hat{A}(t) = \begin{cases} A_0, & 0 \leq t < \underline{D} \\ \mathcal{A}, & t \geq \underline{D} \end{cases}$, $\hat{S}_d(t) = \begin{cases} S_{d0}, & 0 \leq t < \underline{D} \\ \mathcal{S}_d, & t \geq \underline{D} \end{cases}$, and $\hat{D}(t) = \begin{cases} \mathcal{D}_0, & 0 \leq t < t_f \\ \mathcal{D}, & t \geq t_f \end{cases}$, where $\mathcal{A}, \mathcal{S}_d$ are given in Lemma 10, $\mathcal{D} = \hat{D}(t_f)$ is given in Lemma 11, and $A_0, S_{d0}, \mathcal{D}_0$ are arbitrary initial estimates satisfying Assumptions 1, 3.

Defining the state estimation error as

$$e_o^\top := (\tilde{V}_d, \tilde{X}) = (V_d, X) - (\hat{V}_d, \hat{X}), \quad (88)$$

the dynamics of the extended observer error are given by

$$\dot{e}_o = \underbrace{\begin{pmatrix} S_d & -L_v(t)C \\ \tilde{G} & A - L_x(t)C \end{pmatrix}}_{L(t)} e_o + \underbrace{\begin{pmatrix} \Delta S_d(t) \hat{V}(t) \\ \Delta A(t) \hat{X}(t) + B \Delta U(t) \end{pmatrix}}_{\Delta e(t)}, \quad (89)$$

where $\Delta e(t)$ arises entirely from the parameter identification errors for the system matrices and the time delay, where $\Delta S_d(t) := S_d - \hat{S}_d(t)$, $\Delta A(t) := A - \hat{A}(t)$, $\Delta U(t) := U(t - D) - U(t - \hat{D}(t))$. The observer gains, $L_v(t)$ and $L_x(t)$, are piecewise constant which are defined as

$$L_v(t) = \begin{cases} L_{v,0}, & 0 \leq t < \underline{D} \\ \mathcal{L}_v, & t \geq \underline{D} \end{cases}, \quad L_x(t) = \begin{cases} L_{x,0}, & 0 \leq t < \underline{D} \\ \mathcal{L}_x, & t \geq \underline{D} \end{cases} \quad (90)$$

where the initial observer gains $L_{v,0}, L_{x,0}$ are free design parameters, and $\mathcal{L}_v, \mathcal{L}_x$ are determined by using the estimates $\mathcal{A}, \mathcal{S}_d, \mathcal{D}$ to make the matrix $L(t)$ Hurwitz, denoted as \mathcal{L} .

We present the following lemmas to estimate the upper bound of the observation error, which is required for the subsequent construction of the safe output-feedback controller

Lemma 12: For a square matrix L , we have the following estimate $\|e^{Lt}\| \leq M_L(t)e^{-\delta t}, \forall t \geq 0$ where $\delta = -\max \Re(\text{eig}(L))$, and where $M_L = \|P_1\|_2 \|P_1^{-1}\|^2 > 0$ which is constant when L is diagonalizable, otherwise, $M_L(t) = \|P_1\| \|P_1^{-1}\| \sum_{j=0}^{n_k} \frac{t^j}{j!} > 0$ which is a polynomial in t . The matrix P_1 is invertible, satisfying $L = P_1 \Lambda P_1^{-1}$ where Λ is either a diagonal matrix (if L is diagonalizable) or a Jordan matrix (in which the size of the largest Jordan block is n_k).

Proof: Its proof can be found in [48, Appendix 0.4]. \blacksquare

Defining the observer error norm

$$\Omega_e = |\tilde{X}| + |\tilde{V}_d|, \quad (91)$$

we establish the next lemma.

Lemma 13: For initial data $\hat{X}(0) \in \mathbb{R}^n$, $\hat{V}_d(0) \in \mathbb{R}^{n_d}$, the observer (85)–(87) where the observer gains function $L_v(t)$, $L_x(t)$ are defined by (90), and satisfies that $L(t) = \mathcal{L}, t \geq \underline{D}$ is Hurwitz, the observer error system (89) is well-posed in the sense of $\tilde{X}(0) \in \mathbb{R}^n$, $\tilde{V}_d(0) \in \mathbb{R}^{n_d}$, for $t \in [0, \infty)$. Moreover, the exponential convergence to zero of the observer errors (89) is achieved in the sense that

$$\Omega_e \leq \sqrt{2}\Gamma_{e,1}(t) := \rho_{e_0}(t), \quad 0 \leq t < \underline{D}; \quad (92)$$

$$\Omega_e \leq \sqrt{2}\Gamma_{e,2}(t) := \rho_{e_1}(t), \quad \underline{D} \leq t < t_f; \quad (93)$$

$$\Omega_e \leq \sqrt{2}\Gamma_{e,2}(t_f)M_{\mathcal{L}}(t - t_f)e^{-\delta_{\mathcal{L}}(t-t_f)} := \rho_e(t), \quad t \geq t_f \quad (94)$$

where the observer error bound functions $\Gamma_{e,1}(t)$, $\Gamma_{e,2}(t)$ is defined in (97), (98), respectively, and $M_{\mathcal{L}}$, $\delta_{\mathcal{L}}$ is obtained from applying Lemma 12 to the Hurwitz matrix \mathcal{L} .

Proof: The solution to the observer error ODE (89) can be expressed piecewise as

$$e_o(t) = \begin{cases} e_o(0)e^{L_0 t} + \int_0^t e^{L_0(t-\tau)} \Delta e(\tau) d\tau, & t \in [0, \underline{D}] \\ e_o(\underline{D})e^{\mathcal{L}(t-\underline{D})} + \int_{\underline{D}}^t e^{\mathcal{L}(t-\tau)} \Delta e(\tau) d\tau, & t \in [\underline{D}, t_f] \\ e_o(t_f)e^{\mathcal{L}(t-t_f)}. & t \in [t_f, \infty) \end{cases} \quad (95)$$

Before the parameter estimates converge at t_f , the error dynamics are perturbed by the term $\Delta e(\tau)$. The magnitude of this perturbation is bounded, which can be derived from the known bounds of system parameters A, S_d, D according to Assumptions 1, 3. Using the induced 2-norm, these bounds are defined as $\|\Delta S_d(t)\| \leq \delta_{S_d}$, $\|\Delta A(t)\| \leq \delta_A$, $|\Delta U| \leq \delta_U(t)$, where δ_{S_d} and δ_A are positive constants, and $\delta_U(t)$ is a bounded function representing the error resulting from the delay estimate \hat{D} . By the triangle inequality, the upper bound of the perturbation term $\Delta e(t)$ for $t \in [0, \underline{D}]$ is derived as

$$\begin{aligned} \|\Delta e(t)\| &= \left\| \begin{pmatrix} \Delta S_d(t) \hat{V}(t) \\ \Delta A(t) \hat{X}(t) + B \Delta U \end{pmatrix} \right\| \\ &\leq \|\Delta S_d(t)\| |\hat{V}_d(t)| + \|\Delta A(t)\| |\hat{X}(t)| + |B| |\Delta U| \\ &\leq \delta_{S_d} |\hat{V}_d(t)| + \delta_A |\hat{X}(t)| + b \delta_U(t) := \Gamma_1(t) \end{aligned} \quad (96)$$

which will vanish for $t \geq t_f$. It readily follows from (95) that $e_o(t)$ is bounded with $\hat{X}(0) \in \mathbb{R}^n$, $\hat{V}_d(0) \in \mathbb{R}^{n_d}$, and bounded $\Delta e(t)$ within the finite time $t \in [0, t_f]$. Since the matrix \mathcal{L} is Hurwitz, the error e_o will be exponentially convergent to zero for $t \geq t_f$. The results of well-posedness and exponential convergence to zero are thus established.

Next, we calculate the explicit upper bounds of the observer errors. First, for $t \in [0, \underline{D}]$, utilizing Lemma 12, we bound the matrix $e^{L_0 t}$ over the uncertainty set Θ_1 defined in (13) as $\|e^{L_0 t}\| \leq M_{L_0}(t) e^{-\delta_{L_0} t} \leq \bar{M}_{L_0} e^{-\bar{\delta}_{L_0} t}$, where $\bar{\delta}_{L_0} = -\max_{\theta_1 \in \Theta_1} \max \Re(\text{eig}(L_0(\theta_1)))$ is the worst-case decay rate over all possible parameters in Θ_1 . The gain term $\bar{M}_{L_0}(t)$ depends on the structure of the Jordan decomposition of $L_0(\theta_1)$, that is $\bar{M}_{L_0} = \max_{\theta_1 \in \Theta_1} \|P_1(\theta_1)\| \|P_1^{-1}(\theta_1)\|$ if $L_0(\theta_1)$ is diagonalizable for all $\theta_1 \in \Theta_1$, otherwise $\bar{M}_{L_0} = \max_{\theta_1 \in \Theta_1} \|P_1(\theta_1)\| \|P_1^{-1}(\theta_1)\| \sum_{j=0}^{n_k} \frac{\bar{D}^j}{j!} > 0$ which is a polynomial in t , recalling Lemma 12 with unknown Θ_1 . Accordingly, for the interval $t \in [0, \underline{D}]$, we establish the upper bound for the error state norm $|e_o(t)|$ as

$$\begin{aligned} |e_o(t)| &\leq M_0 \bar{M}_{L_0} e^{-\bar{\delta}_{L_0} t} \\ &+ \int_0^t \bar{M}_{L_0} e^{-\bar{\delta}_{L_0}(t-\tau)} \Gamma_1(\tau) d\tau := \Gamma_{e,1}(t), \end{aligned} \quad (97)$$

where the constant $M_0 = \sqrt{\sum_{i=1}^{\bar{n}} (\bar{\zeta}_{0,i} - \underline{\zeta}_{0,i})^2}$ is the upper bound on the initial observer error $|e_o(0)|$ which derived from the known upper bound $\bar{\zeta}_{0,i}$ and lower bound $\underline{\zeta}_{0,i}$ of each entry in the initial state vectors in Assumption 8. Next, recalling Lemma 10, we know that the error term $\Delta S_d(t) = 0$, $\Delta A(t) = 0$ after $t \geq \underline{D}$. It implies that the parameter estimation error term $\Delta e(t)$ in (89) becomes $(0 \ B \Delta U(t))^\top$ after $t > \underline{D}$, and thus the upper bound of the perturbation term $\Delta e(t)$ becomes

$\|\Delta e(t)\| \leq b \delta_U(t) := \Gamma_2(t)$, $t \in [\underline{D}, t_f]$. The upper bound of the whole error state $|e_o(t)|$ for $t \in [\underline{D}, t_f]$ is derived as

$$\begin{aligned} |e_o(t)| &\leq \Gamma_{e,1}(\underline{D}) M_{\mathcal{L}}(t - \underline{D}) e^{-\delta_{\mathcal{L}}(t-\underline{D})} \\ &+ \int_{\underline{D}}^t M_{\mathcal{L}}(t-\tau) e^{-\delta_{\mathcal{L}}(t-\tau)} \Gamma_2(\tau) d\tau := \Gamma_{e,2}(t), \end{aligned} \quad (98)$$

where $M_{\mathcal{L}}(t)$, $\delta_{\mathcal{L}} > 0$ are obtained by applying the result of lemma 12 to the Hurwitz matrix \mathcal{L} . Finally, for $t \geq t_f$, we have $\Delta U(t) = 0$ from Lemma 11, such that $\Delta e(t) = 0$. Thus, the upper bound of the observer error is derived as $|e_o(t)| \leq \Gamma_{e,2}(t_f) M_{\mathcal{L}}(t - t_f) e^{-\delta_{\mathcal{L}}(t-t_f)}$ for $t \in [t_f, \infty)$. Recalling Ω_e defined in (91), applying Young's inequality yields the following bound $\Omega_e \leq \sqrt{2} |e_o(t)|$. ■

C. Safe output regulation under unknown parameters

Leveraging the above data-driven identification, we now design the safe output regulator. With the modified dynamic matrices A, S_d in (70), the first transformation (17) in Sec. III-A.1 reduces to $Z(t) = X(t) + T_v V(t)$. The subsequent transformation design then proceeds as described in Sec. III-A. With the estimates $\hat{X}(t)$ and $\hat{V}(t)$ from the observer (85)–(87), we can construct the output-feedback controller:

$$\hat{U}_d(t) := \mathcal{U}(\hat{X}(t); \hat{\Theta}(t)) + \vartheta_0 \hat{\rho}_e(t; \hat{\Theta}(t)), \quad (99)$$

where $\mathcal{U}(\hat{X}(t); \Theta)$ is derived by employing the observer state $\hat{X}(t) = (\hat{V}_d(t), V_r(t), \hat{X}(t))$ to replace the system state (26) in (34). Following the approach in [48], the following function $\hat{\rho}_e(t)$ with the known constant ϑ_0 given by (68) is added in (99) to tolerate the observer error (88),

$$\hat{\rho}_e(t) = \begin{cases} 0, 0 \leq t < t_f \\ 2 \max \{ \|\tilde{K} e^{\mathcal{D} \mathcal{A}}\|, |\bar{\gamma}(1, \hat{\Theta}(t_f))|, \xi_e \} \rho_e(t), t \geq t_f \end{cases} \quad (100)$$

where the gains \tilde{K} and $\bar{\gamma}(1, \hat{\Theta}(t_f))$ are obtained by substituting $\hat{\Theta}(t_f)$ into (20) and (A.1), $\rho_e(t)$ is given in (94), and where ξ_e is a constant defined in Assumption 9.

Defining the vector ζ_0 that includes the initial states $X(0)$ and $V_d(0)$, it belongs in the set $\bar{\zeta}_0$ according to Assumption 8. The vector θ_1, \mathfrak{D} represents the unknown system parameters, bounded by $\bar{\Theta}_1, D_0$ from Assumptions 3, 1. On the basis of it, we substitute the lower bound $\underline{h} = \min_{\zeta_0 \in \bar{\zeta}_0, \theta_1 \in \bar{\Theta}_1, \mathfrak{D} \in D_0} \mathcal{P}_0(\zeta_0; \theta_1, \mathfrak{D})$ into (65) for the uncertain value $h(e(D), D)$, to choose the positive constant ϵ in (65) to ensure that $h_1(z_1(D), D) \geq 0$.

Analogously, the design parameters k_i are selected only using the boundaries to robustly guarantee the initial positivity of all functions $h_i(z_i(D), D)$ across the entire uncertainty set, i.e.,

$$k_i \geq \max_{\zeta_0 \in \bar{\zeta}_0, \theta_1 \in \bar{\Theta}_1, \mathfrak{D} \in D_0} \{0, \hat{k}_i(\zeta_0; \theta_1, \mathfrak{D})\}, i = 1, \dots, n-1, \quad (101)$$

$k_n \geq 0$, where \hat{k}_i is given by (37).

Following the same design principles as between (66)–(68), we formulate the following safe controller to operate under

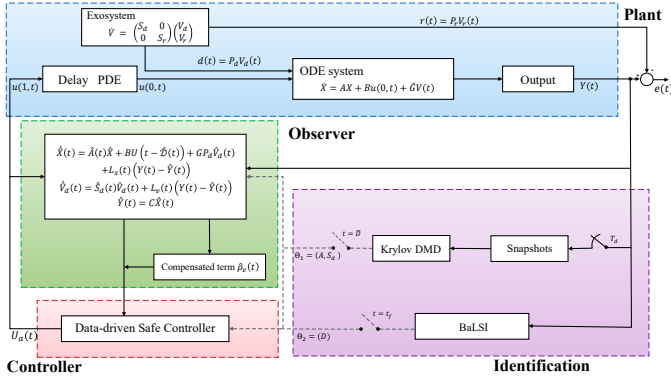


Fig. 2: Diagram of the proposed output-feedback data-driven safe control system.

both parameter and state uncertainty:

$$U_a(t) = \begin{cases} \max_{\zeta(t) \in \bar{\zeta}(t), \theta_1 \in \bar{\Theta}_1, \mathcal{D} \in D_0} \vartheta_0 \mathcal{U}(\zeta(t); \theta_1, \mathcal{D}), & 0 \leq t < \underline{D} \\ \max_{\zeta(t) \in \bar{\zeta}(t), \mathcal{D} \in D_0} \vartheta_0 \mathcal{U}(\zeta(t); \hat{\Theta}_1(\underline{D}), \mathcal{D}), & \underline{D} \leq t < t_f, \\ \hat{U}_d(t), & t \geq t_f \end{cases} \quad (102)$$

where the form of \mathcal{U} is specified by (34), and $\bar{\zeta}(t)$ denotes all possible values of states, obtained from the observer state $\hat{\chi}(t)$ with its upper bound defined in (92), (93), i.e.,

$$\bar{\zeta}(t) = \begin{cases} \{\zeta(t) \in \mathbb{R}^{\bar{n}} : |\zeta(t) - \hat{\chi}(t)| \leq \rho_{e_0}(t)\}, & 0 \leq t < \underline{D} \\ \{\zeta(t) \in \mathbb{R}^{\bar{n}} : |\zeta(t) - \hat{\chi}(t)| \leq \rho_{e_1}(t)\}, & \underline{D} \leq t < t_f \end{cases} \quad (103)$$

Remark 2: To strictly guarantee system safety over the time interval $[0, t_f]$ under unknown states and parameters, all possible values are computed. This process is potentially computationally demanding. However, if a control input that guarantees safety over the finite horizon $[0, \underline{D}]$ is known, the computational burden can be significantly reduced by simply applying this safe input during this initial interval. Such an input for a short initial time is always available in many practical applications.

The diagram of the proposed safe output regulation closed-loop system is depicted in Fig. 2, and the result is presented in the next subsection.

D. Result of safe output-feedback Controller

Theorem 2: For initial data $X(0) \in \mathbb{R}^n$, $V(0) \in \mathbb{R}^{n_v}$, $\hat{X}(0) \in \mathbb{R}^n$, $\hat{V}(0) \in \mathbb{R}^{n_v}$ satisfying Assumption 8, and the safety constraint $h(e, t)$ satisfying Assumptions 4, 7, 9, choosing the design parameters k_1, \dots, k_n satisfying (101), the closed-loop system consisting of the disturbed linear plant (1), (2) with unknown Θ (71), the observer (85)–(87), and the controller (102), has the following properties:

- 1) There exists a unique solution $X(t) \in \mathbb{R}^n$, $V(t) \in \mathbb{R}^{n_v}$, $u[t] \in L^2(0, 1)$.
- 2) The identification $\hat{\Theta}(t)$ of unknown parameters Θ is bounded and reaches the true value in finite time t_f that is defined in (84).

3) Tracking error state $e(t)$ (14) is convergent to zero and all states are bounded;

4) Safety is ensured in the sense that

a) If the initial safe condition in Definition 1 is met, then safety is guaranteed for $t \in [0, \infty)$.

b) If the initial safe condition in Definition 1 is not met, but $h(e(D), D) > 0$, then safety is guaranteed for $t \geq D$.

c) If the initial safe condition in Definition 1 is not met, and $h(e(D), D) \leq 0$, the safety is guaranteed for $t \geq D + \bar{t}$ where $\bar{t} > 0$ can be arbitrarily assigned by users.

Proof: 1) From the initial condition (8) and the transformations (17), (22), (23), as well as the exogenous signal model (6), we have $w[0] \in L^2(0, 1)$, $H(0) \in \mathbb{R}^n$, and $V(t) \in \mathbb{R}^{n_v}$. On the interval $t \in [0, t_f]$, define the difference between $U_a(t)$ (102) and $U(t)$ (34) as: $\hat{\eta}_1(t) = U_a(t) - U(t)$, which arises from both parameter mismatch and state estimation error. A fundamental property of linear systems guarantees that for bounded inputs, $\hat{\eta}_1(t)$ remains bounded on a finite horizon $t \in [0, t_f]$. Note that, for the time period $t \in [0, t_f]$, the target system becomes (31), (32) with $w(1, t) = \hat{\eta}_1(t)$. Thus, we have that $w(1, t)^2$ is bounded during $t \in [0, t_f]$. According to Lemmas 10, 11, all identified parameters have converged to their true values by the time $t = t_f$. Consequently, when the controller (102) switches at $t = t_f$ with the exact identification $\hat{\Theta}(t_f)$, the difference between the applied controller $U_a(t)$ (102) and the nominal controller $U(t)$ (34) is given by $U_a(t) - U = \vartheta_0 \hat{\rho}_e(t; \hat{\Theta}(t_f)) + \hat{\eta}_2(t)$, where $\hat{\eta}_2(t)$ is defined as

$$\begin{aligned} \hat{\eta}_2(t) &= \mathcal{U}(\hat{\chi}(t); \hat{\Theta}(t_f)) - U \\ &= \tilde{K} e^{\mathcal{D} \mathcal{A}} X(t) - \bar{\gamma}(1; \hat{\Theta}(t_f)) V(t) - \tilde{\mathcal{P}}(V(t), X(t)). \end{aligned} \quad (104)$$

Accordingly, the target system becomes (31), (32) with

$$w(1, t) = \vartheta_0 \hat{\rho}_e(t) + \hat{\eta}_2(t), \quad t \geq t_f. \quad (105)$$

Recalling Lemma 13, (35), (72) in Assumption 9, (100), we know that $w(1, t)$ is bounded for all $t \in [t_f, \infty)$ from (105). As it is also bounded on $[0, t_f]$, $w(1, t)$ is bounded for $t \geq 0$, which ensures $w[t] \in L^2(0, 1)$. Following the same process in the proof of property 1) in Theorem 1, we have $H(t) \in \mathbb{R}^n$, $Z(t) \in \mathbb{R}^n$, $X(t) \in \mathbb{R}^n$ and $u[t] \in L^2(0, 1)$ as well. Recalling the results about the observer errors in Lemma 13, and (88), Property 1 is obtained.

2) According to Lemmas 10, 11, we directly obtain the property 2) that the parameter identification $\hat{\Theta}(t)$ achieves the true value in finite time t_f .

3) Combining Lemma 13 with (35) and (72) from Assumption 9 yields the bound of $\hat{\eta}_2(t)$ in (104) as

$$|\hat{\eta}_2(t)| \leq 2 \max\{\|\tilde{K} e^{\mathcal{D} \mathcal{A}}\|, |\bar{\gamma}(1, \hat{\Theta})|, \xi_e\} \Omega_e \leq \hat{\rho}_e(t). \quad (106)$$

As established in Lemma 13 via (94), $\rho_e(t)$ converges exponentially to zero. This implies that $\hat{\rho}_e(t)$, as defined in (100), and $w(1, t)$, as given by (105), also converge exponentially to zero. Follow the same process in the proof of the property 3) in Theorem 1, this property is obtained.

4) From Assumption 4, we have $\text{sgn}(\vartheta(t)) \equiv \text{sgn}(\vartheta_0)$. Based on $\hat{\eta}_1$, (102), this implies that $b\vartheta(t)w(0, t) \geq 0$ for $t \in [D, D + t_f]$. Furthermore, combining (106) with (105), it shows that the product $b\vartheta(t)w(0, t)$ remains non-negative for

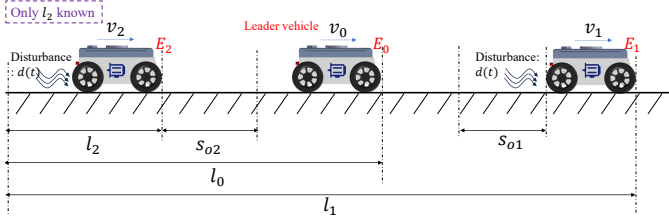


Fig. 3: Vehicle platooning with leader E_0 , and the controlled $E_i, i = 1, 2$, where the safe s to be maintained are s_{oi} .

all $t \geq D + t_f$. Consequently, we conclude that $b\vartheta w(0, t) \geq 0$ for all $t \in [D, \infty)$, regardless of the sign of ϑ . The selection of the design parameters k_i in (101) defines a stricter subset of the conditions in (36), which strictly guarantees the positivity of the initial barrier function values, i.e., $h_i(\underline{z}_i(D), D)$. Thus, the result of Lemma 1 remains valid. Following the same procedure used to prove property 4) in Theorem 1, we obtain this property. The proof of this theorem is complete. \blacksquare

V. APPLICATION IN SAFE VEHICLE PLATOONING

A. Physical model

In this section, we validate the effectiveness of the designed controller through a practical application of safe vehicle platooning, depicted in Fig. 3, which consists of three vehicles, where the middle vehicle, E_0 , serves as a reference, traveling at a known speed $v_0(t)$. The control actions are applied to the other two vehicles: the preceding vehicle, E_1 , and the following vehicle, E_2 . Each vehicle E_i is subject to an unknown input delay D_i between the control command $F_i(t)$ and the actual drive force $F_{w,i}(t)$, accounting for actuator dynamics and communication latency, i.e., $F_{w,i}(t) = F_i(t - D_i)$. According to Newtonian mechanics, the longitudinal dynamics of the i -th vehicle are described by:

$$\frac{dl_i}{dt} = v_i(t) + d_i(t), \quad M_i \frac{dv_i}{dt} = F_{w,i}(t) - F_r + d_i(t), \quad (107)$$

where M_i is the mass of vehicle E_i , $l_i(t)$ and $v_i(t)$ are its displacement and speed respectively, and $F_r = f_1 v_i(t)$ represents the overall resistance force. The exogenous signal $d(t) = (d_1(t), d_2(t))^\top$ is introduced to capture the influence of external disturbances, such as wind gusts and road slope, as well as unmodeled dynamics and modeling errors.

Considering the disturbance $d(t)$ and target trajectory $r_i(t)$ are both generated by an exosystem $\dot{V}(t) = SV(t)$ with $S = \text{diag}(S_d, S_r)$ and $V_i(t) = (V_d(t), V_{r,i}(t))^\top$ according to (4)–(7) and defining the state vector as $X_i(t) = (l_i(t), v_i(t))^\top$, and the control input as $U_i(t) = F_i(t)$, the vehicle dynamics system can be expressed in state-space form:

$$\dot{X}_i(t) = \begin{pmatrix} 0 & 1 \\ 0 & a_i \end{pmatrix} X_i(t) + \bar{G} V_i(t) + \begin{pmatrix} 0 \\ b_i \end{pmatrix} U_i(t - D_i). \quad (108)$$

Here, the disturbance part of exosystem $V(t)$ is generated by $S_d = (0 \ 1; \beta_1 \ 0)$, $P_d = I_2$ recalling (4). This signal affects the vehicle dynamics through the input matrix $\bar{G} = G \bar{P}_d$, where $G = (1 \ 1; 0 \ 1)$ and $\bar{P}_d = (P_d, 0)$. Besides, the specified reference trajectory for each vehicle E_i is $r_i(t) =$

TABLE I: Parameters and Uncertainty Bounds

Parameter	values	Bounds
Linear damping coefficient: f_1	5 (Ns/m)	–
Vehicle mass: M_1	5 (kg)	–
Vehicle mass: M_2	4 (kg)	–
Input delay in E_1 : D_1	1.5 (s)	[1, 3]
Input delay in E_2 : D_2	1.2 (s)	[1, 3]
Input parameters b_i	$1/M_i$	[0.1, 1]
system parameters a_i	$-f_1/M_i$	[-2, 0]
Disturbance parameter: β_1	$-1/4$	[-1, 0]

$l_0(t) + (-1)^{i-1} s_{oi}$, where s_{oi} denote the preset target distance. The leader's displacement is given by $l_0(t) = 4t - \cos(t) + 11$. This trajectory is produced by the reference generator from (5), defined by $S_r = (0, 1, 0, 0; 0, 0, 1, 0; 0, -1, 0, 1; 0, 0, 0, 0)$, $P_r = (1, 0, 0, 0)$, with the initial condition $V_{r,i}(0) = (10 + (-1)^{i-1} s_{oi}, 4, 1, 4)^\top$.

The model parameters are not precisely known which arise from various operational factors, including variations in vehicle load and unpredictable network latencies. We assume that these unknown parameters are bounded within known intervals, as shown in Table I.

B. Control objective

The objective is to enforce a safe platoon formation by regulating the distances between adjacent vehicles, defined as $s_1(t) = l_1(t) - l_0(t)$ and $s_2(t) = l_0(t) - l_2(t)$, to their designated safe setpoints, s_{01} and s_{02} , without breaching the safety constraint. If starting from an unsafe condition, i.e., $s_i(D) < s_{oi}$, the system is expected to return to the safe region in a finite time assigned by users, and subsequently converge to the specified setpoints without breaching safe constraints.

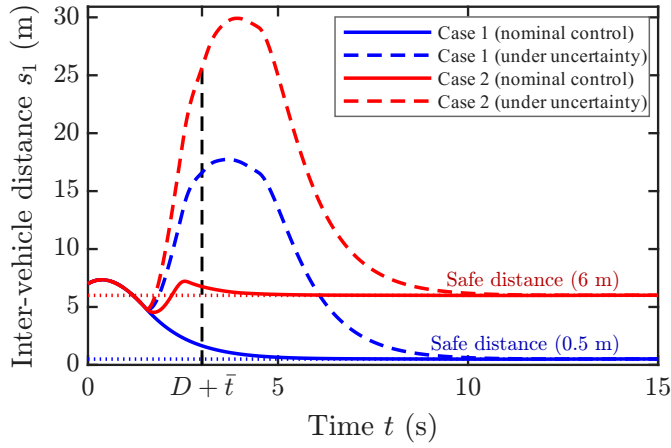
Front vehicle E_1 : The safety constraint for the front vehicle is formulated as the barrier function: $\mathcal{H}_1(e_1(t), t) = X_{1,1}(t) - r_1(t) = e_1(t) \geq 0$. For this vehicle, all states, including disturbance states, are assumed to be available to test the performance of the control design in Sec. III.

Rear vehicle E_2 : The safety constraint is formulated as the barrier function: $\mathcal{H}_2(e_2(t), t) = r_2(t) - Y(t) = -e_2(t) \geq 0$. It is obtained from (27) that $\vartheta_2 = -1$. For this vehicle, only the output state $Y(t) = x_{2,1}$ is available, to test the performance of the control design in Sec. IV.

C. Controller design

The control gains are selected as $k_1 = 3$ and $k_2 = 1$ according to (36), (37), (66), (101), with the initial distances $x_{1,1}(0) = 17$, $x_{2,1}(0) = 5$ and the initial velocities of $x_{i,2}(0) = 5$ m/s. The initial value of the disturbance is $V_d(0) = (1, 0)^\top$. Based on the derived controller (34), the control gains for vehicles E_i are calculated as: $K_i = \frac{1}{b_i}(0, a_i)$, $G_{0i} = \frac{1}{b_i}(g_2 + g_1 S_i - P_r S_i^2)$, $f_i = -\frac{1}{b_i}((k_1 + k_2) Z_{2,i} + k_1 k_2 Z_{1,i})$

1) Case1: Within safe region initially: To verify the safety and convergence properties, the target distances are set as the smaller value $s_{01} = 0.5$ and $s_{02} = 0.5$. According to (34), the

Fig. 4: Distance between vehicles E_1 and E_0 .

nominal controller for each vehicle E_i is

$$U_i(t) = -\frac{1}{b} [k_1 k_2 x_{i,1}(t+D) + (k_1 + k_2 + a_i)x_{i,2}(t+D) + ((k_1 + k_2)g_1 + g_2 + g_1 S - (k_1 k_2 \bar{P}_r + (k_1 + k_2) \bar{P}_r S_r + \bar{P}_r S^2)) e^S V(t)] \quad (109)$$

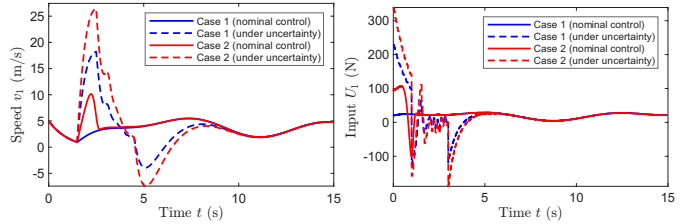
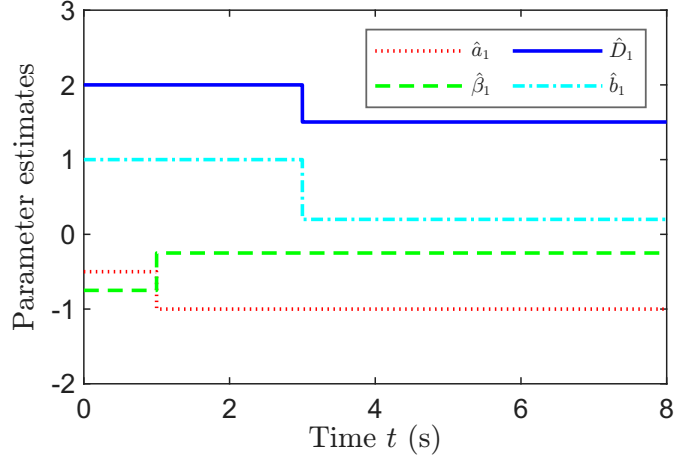
with the prediction $X_i(t+D)$ given by (21). Considering the system parameter uncertainties $\Theta = \{a_1, \beta_1, b_1, D_1\}$, according to (67), the data-driven safe controller is derived from the nominal controller (109) based on the control design in Sec. III-D. Besides, for vehicle E_2 , only the output state $Y(t) = x_{2,1}(t)$ is measurable and the system parameters $\Theta = \{a_2, \beta_2, D_2\}$ are unknown, thus the observer (85)–(87) is implemented to estimate the full state $X_2(t), V_d(t)$. Using the estimated state $\hat{X}_2(t), \hat{V}_d(t)$ replacing the state $X_2(t), V_d(t)$ in (109), and added the compensated term $\hat{\rho}_e(t; \hat{\Theta}(t))$ in (100) to mitigate the effects of observer error and parameter estimation error, according to Sec. IV-C. The observer gains are selected as $L_{v,0} = 0$, $\mathcal{L}_v = (-0.6, 15)^\top$, $L_{x,0} = 0$, $\mathcal{L}_x = (9, 10)^\top$ recalling (90). Besides, the known bound of unknown states is given by $x_{2,2} \in [2, 6]$ and $V_{d,i} \in [-2, 2]$ satisfying Assumptions 8, and we take $\hat{x}_{2,2} = 2$ and $\hat{V}_d = 0$ as the initial values of the observer.

2) Case2: Within unsafe region initially: Here, the target distances are set as larger values $s_{o1} = 12$ and $s_{o2} = 8$, where the barrier function $\mathcal{H}_i(e_i(D), D) < 0$, which are initially unsafe. Considering $\varsigma_i(t)$ given by (24), (65), with design parameters $\bar{t} = 1.5, \epsilon = 5$, there is an additional term $\bar{\varsigma}_i(t) = -\frac{1}{b\vartheta_i} (k_1 k_2 \varsigma_i(t+D) + (k_1 + k_2) \dot{\varsigma}_i(t+D) + \ddot{\varsigma}_i(t+D))$ added in (109).

For output-feedback systems, the compensation term $\hat{\rho}_e(t; \hat{\Theta}(t))$ is computed using observer error bounds, i.e., $\rho_{e_0}(t), \rho_{e_1}(t)$ from (92), (93). Following parameter identification at t_f , the state observer can be re-initialized with the current state estimates $(\hat{X}(t_f), \hat{V}_d(t_f))$ and updated using the now-identified system model. This can reduce conservatism at the cost of an increased computational burden.

D. Simulation results

The simulation, including Cases 1 and 2, is performed using the finite difference method with a time step $dt = 0.001$ and

Fig. 5: Speed and Control force of vehicle E_1 .Fig. 6: Estimates of the unknown parameters (a_1, β_1, b_1, D_1) in vehicle E_1 .

a space step $dx = 0.01$. The iteration interval for unknown parameters is taken as $d_D = 0.1$.

The simulation results of vehicle E_1 are shown in Figs. 4–6, where the blue line represents the results in Case 1, and the red line represents the results in Case 2. The solid lines denote the nominal control (34), while dashed lines denote the proposed data-driven safe control (67). As shown in Fig. 4, the distance between vehicles E_1 and E_0 converges to the desired distance ($s_{o1} = 0.5$ m in Case 1, $s_{o1} = 6$ m in Case 2). Moreover, in Case 1, the safe distance is ensured all the time. In Case 2, from an unsafe vehicle distance at $t = D$, i.e., the distance between the vehicles is less than the desired distance, vehicle distance is driven back and maintained in the safe distance within the predefined time $D + \bar{t}$. The vehicle's speed and control input are illustrated in Figs. 5a, 5b, respectively. Fig. 6 demonstrates that all unknown parameters $\{a_1, \beta_1, b_1, D_1\}$ converge to their true values within the finite time $t_f = 3$ s.

The simulation results of vehicle E_2 are shown in Figs. 7–9. As illustrated by the blue line in Fig. 7, the inter-vehicle distance converges to the desired safe distance $s_{o2} = 0.5$ m without breaching the safety constraint in Case 1. The red line in Fig. 7 for Case 2 shows that, starting from an unsafe initial distance, the inter-vehicle distance is regulated to the safe region by the preset time $D + \bar{t}$, and then safely converges to the desired distance $s_{o2} = 8$ m. The results of the speed $v_2(t)$ and control force $U_2(t)$ are illustrated in Figs. 8a, 8b. The observer successfully estimates the true system states, as shown in Figs. 9a, 9b, and the disturbance states, as shown in

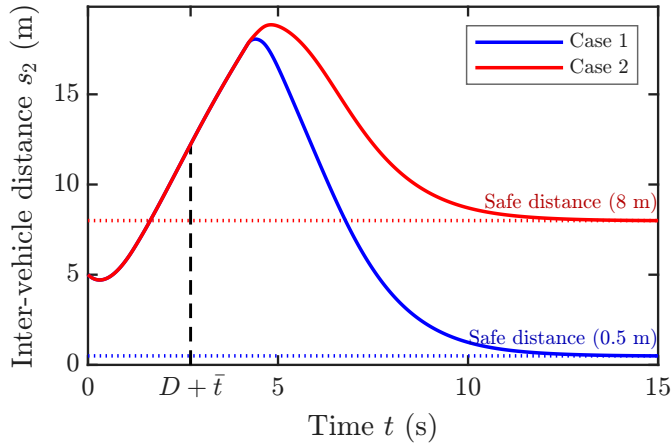
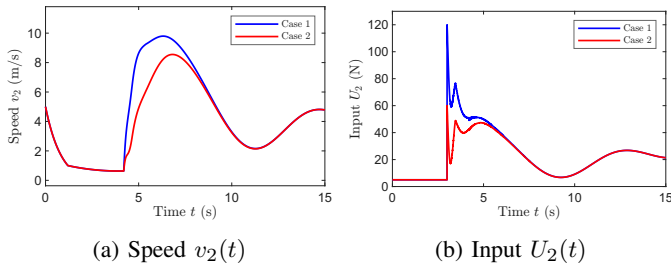
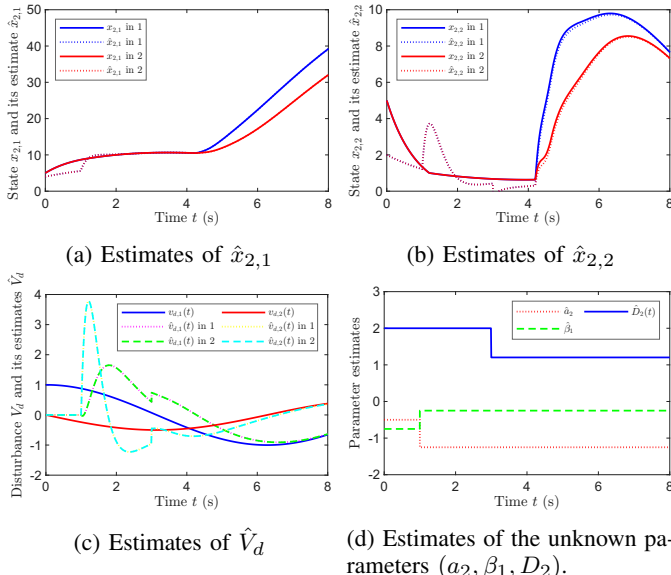
Fig. 7: Distance between vehicles E_2 and E_0 .Fig. 8: Speed and Control force of vehicle E_2 .

Fig. 9: Estimates of states and parameters.

Fig. 9c. The unknown parameters $\{a_2, \beta_1, D_2\}$ in vehicle E_2 are exactly identified within the finite time $t_f = 3$ s, as shown in Fig. 9d.

VI. CONCLUSION AND FUTURE WORK

This paper investigated the safe output regulation problem for strict-feedback linear systems, addressing challenges posed by substantial uncertainties, including unknown input delay, uncertain system dynamics, and external disturbances. A

novel, data-driven, safe delay-compensated control design was developed by integrating a delay compensation mechanism, a Krylov DMD and BaLSI adaptive identifier, and a safety filter. For the more challenging scenario where only the furthest state as output is measurable, an observer was designed to estimate the unmeasured states and disturbances. Based on this, the output-feedback control scheme was constructed. The proposed control design guarantees that the output of the closed-loop system safely tracks the target trajectory, all states are bounded, and all unknown parameters are identified exactly in finite time. An application in safe vehicle platooning was presented to validate the theoretical results.

Future research will focus on extending the current results to systems with more stochastic uncertainties, such as stochastic noise and disturbance, and exploring the experimental validation of the proposed control scheme on practical systems.

APPENDIX

A. The calculation of the PDE transformation (30) and its inverse transformation

Substituting the time and spatial derivatives of the transformation (30) into (32), and requiring the resulting identity to hold for all u , $X(t)$, and $V(t)$, yields the following conditions: $-q_x(x, y) = q_y(x, y)$, $q(x, 0) = D\gamma(x)B$, $\dot{\gamma}(x) = D\gamma(x)A$, $\dot{\gamma}(x) = D\bar{\gamma}(x)S + D\gamma(x)\bar{G}$, $D\psi_t = \psi_x$. Comparing (28) with (31) yields the boundary condition $w(0, t) = u(0, t) + \frac{1}{\vartheta}f(\bar{z}_n(t), t) - \frac{1}{b}(\sigma_n + \bar{P}_r S^n)V(t) + KX(t)$. By setting $t = 0$ in (30) and comparing the result with the boundary condition above, we obtain the initial conditions $\gamma(0) = -K$, $\bar{\gamma}(0) = \frac{1}{b}(\sigma_n + \bar{P}_r S^n)$, $\psi(0, t) = \frac{-1}{\vartheta(z_1(t), t)}f(\bar{z}_n(t), t)$. Solving the ODEs γ , $\bar{\gamma}$ with the above initial conditions yields $\gamma(x) = -Ke^{DAx}$,

$$\bar{\gamma}(x) = - \int_0^x DKe^{DAy} \bar{G} e^{DS(x-y)} dy + \frac{1}{b}(\sigma_n + \bar{P}_r S^n) e^{DSx}. \quad (\text{A.1})$$

Finally, considering the general solution $Q(x-y)$ to $q(x, y)$, $\bar{\psi}(t - D + Dx)$ to ψ , we get

$$q(x, y) = -KDBe^{DA(x-y)}, \quad (\text{A.2})$$

$$\psi(x, t) = -\frac{f(\bar{z}_n(t + Dx), t + Dx)}{\vartheta(z_1(t + Dx), t + Dx)}. \quad (\text{A.3})$$

The inverse transformation of (30) is given by:

$$u(x, t) = w(x, t) + \int_0^x \bar{q}(x, y)w(y, t) dy + \gamma_1(x)X(t) + \bar{\gamma}_1(x)V(t) + \psi_1(x, t). \quad (\text{A.4})$$

Through similar calculations, its components are explicitly solved as $\bar{q}(x, y) = -DKBe^{D(A-BK)(x-y)}$, $\gamma_1(x) = -Ke^{D(A-BK)x}$, and $\bar{\gamma}_1(x) = -G_0e^{DSx} + \int_0^x D\gamma_1(y)(\bar{G} - BG_0)e^{DS(x-y)} dy$. The remaining term, $\psi_1(x, t)$, is calculated based on $\gamma_1(x)$ and $\psi(x, t)$.

B. The proof of Lemma 1

Setting $t = D$ in (23), then one gets

$$\begin{aligned} h_{i+1}(z_{i+1}(D), D) &= \sum_{j=1}^i \frac{\partial h_i}{\partial z_j} z_{j+1}(D) + \frac{\partial h_i}{\partial t} \\ &\quad + k_i h_i(z_i(D), D). \end{aligned} \quad (\text{B.1})$$

The above recursive formula (B.1) is used to establish the inductive step : if $h_i(z_i(D), D)$, then $h_{i+1}(z_{i+1}(D), D)$ under the selection of parameters k_i in (36), (37). The base case, $h_1(z_1(D), D) > 0$, is guaranteed by (22), (24). It thus follows by induction that $h_i(z_i(D), D) \geq 0$ for all $i = 1, \dots, n$. Given these safe initial conditions and $w[t] \equiv 0$ for $t \geq D$, the system structure described by (31)–(33) guarantees that non-negativity is maintained for all subsequent times, i.e., $h_i(z_i(t), t) \geq 0$ for all $t \in [D, \infty]$ and $i = 1, \dots, n$.

C. The proof of Lemma 2

Considering the boundedness of ϑ (27) concluded from Assumption 4, we know that $w[t]$, $H(t)$ are bounded all the time from the target system (31)–(33) utilizing the method of characteristics. Especially, the matrix A_h is Hurwitz above the selection of k_i (36) and $w[t] \equiv 0$ for $t \geq D$, which further indicates that $|H(t)|$ is exponentially convergent to zero. From (22), (24), Assumption 4 and the boundedness of h_1 , we obtain that $z_1(t) = e(t)$ is bounded. Differentiating (23) with respect to z_{i-1} , we have $\frac{\partial h_i}{\partial z_{i-1}} = \frac{\partial h_{i-1}}{\partial z_{i-2}} + \frac{\partial^2 h_{i-1}}{\partial z_{i-1} \partial t} + k_{i-1} \frac{\partial h_{i-1}}{\partial z_{i-1}} = \frac{\partial h_{i-1}}{\partial z_{i-2}} + \frac{\partial^2 h_1}{\partial z_1 \partial t} + k_{i-1} \frac{\partial h_1}{\partial z_1}$. Beginning from $\frac{\partial h_2}{\partial z_1} = \frac{\partial^2 h_1}{\partial z_1 \partial t} + k_1 \frac{\partial h_1}{\partial z_1}$, we obtain that $\frac{\partial h_2}{\partial z_{i-1}} = \frac{\partial h_1}{\partial z_1} \sum_{j=1}^{i-1} k_j + (i-1) \frac{\partial h_1}{\partial z_1 \partial t}$, $\forall i \geq 2$ from the induction step. Recursively, we obtain $\sum_{i=1}^n \sum_{j=1}^i \frac{|\partial h_i|}{\partial z_j} \leq \mathcal{M}(|\frac{\partial h_1}{\partial z_1}| + \sum_{j=1}^{n-1} |\frac{\partial h_1}{\partial z_1 \partial t^{n-1}}|)$ for some positive constant \mathcal{M} . Since ς has continuous derivatives of all orders recalling (22), (24) and Assumption 4, it further indicates that all $\frac{\partial h_i}{\partial z_j}$, $1 \leq j \leq i \leq n, i, j \in \mathbb{N}$ are bounded. The boundedness of $Z(t)$ is obtained from the boundedness of $\frac{\partial h_i}{\partial z_j}, H(t)$. Next, we have the boundedness of $|X(t)|$ from (17), together with the boundedness of $V(t)$ from (6). Applying the Cauchy-Schwarz inequality to the inverse transformation (A.4) given in Appendix A, we have that $u[t]$ is bounded. Especially, as defined in (24), $\varsigma \equiv 0$ is ensured after a finite time $t = D + \bar{t}$, regardless of which case applies. Thus, we know that $e(t)$ is exponentially convergent to zero from the exponential convergence to zero of $h_1(z_1(t), t)$, recalling (22) and Assumption 4. The proof is complete.

D. The proof of Lemma 3

It readily follows from (46) that $\text{rank } Q_o = \tilde{n}$. Since (\tilde{A}, I) is controllable and \tilde{A} is cyclic from Assumption 5, we know that $(\tilde{A}, \tilde{X}(0))$ is controllable for almost all $\tilde{X}(0) \in \mathbb{R}^{\tilde{n}}$. It indicates that $\text{rank } Q_c = \tilde{n}$ given in (47) with Assumption 6. Applying Sylvester's rank inequality and Rank of product inequality to (45), we know that $\text{rank } H_{\tilde{n}}(\tilde{X}) = \tilde{n}$. The proof is complete.

E. The proof of Lemma 5

Applying (45) with (49), (50) yields that $Q_o Q_c f = -Q_o \tilde{A}_d^{\tilde{n}} \tilde{X}(0)$, which is equivalent to

$$Q_o(Q_c f + \tilde{A}_d^{\tilde{n}} \tilde{X}(0)) = 0. \quad (\text{E.1})$$

Given that $\text{rank } H_{\tilde{n}}(\tilde{X}) = \tilde{n}$, the observability matrix Q_o has full column rank, i.e., $\text{rank}(Q_o) = \tilde{n}$ and $\text{rank } Q_c = \tilde{n}$ as well. Therefore, Q_o has a trivial null space, such that $Q_c f + \tilde{A}_d^{\tilde{n}} \tilde{X}(0) = 0$ only holds for (E.1) and has a unique solution because $\det Q_c \neq 0$. Combining with (47), rearranging gives

$$P_F(\tilde{A}_d) \tilde{X}(0) = 0, \quad (\text{E.2})$$

where $P_F(\tilde{A}_d) = (\tilde{A}_d^{\tilde{n}} + f_{\tilde{n}-1} \tilde{A}_d^{\tilde{n}-1} + \dots + f_1 \tilde{A}_d + f_0 I)$ and $P_F(\lambda) = \det(\lambda I - F)$ denotes the characteristic polynomial of the companion matrix F given in (49). According to Assumption 5, the eigenvectors $\tilde{\nu}_i$ are linearly independent, so the matrix \tilde{V} is invertible. Using the eigendecomposition of the system, $\tilde{A}_d = \tilde{V} \hat{\Lambda} \tilde{V}^{-1}$ and $\tilde{X}(0) = \tilde{V} \tilde{\varphi}(\tilde{X}(0))$ from (40), we can rewrite (E.2) as

$$\tilde{V} P_F(\hat{\Lambda}) \tilde{V}^{-1} \tilde{V} \tilde{\varphi}(\tilde{X}(0)) = \tilde{V} P_F(\hat{\Lambda}) \tilde{\varphi}(\tilde{X}(0)) = 0, \quad (\text{E.3})$$

where $\hat{\Lambda} = \text{diag}(\hat{\lambda}_1, \dots, \hat{\lambda}_n)$. Because $\det Q_c \neq 0$ and $\det \tilde{V} \neq 0$, we know that $\tilde{\varphi}_i(\tilde{X}(0)) \neq 0, i = 1, \dots, \tilde{n}$ by using the PBH eigenvector tests in (39), such that only $P_F(\hat{\Lambda}) = 0$ can hold in (E.3). Therefore, the eigenvalues of \tilde{A}_d are identical to the eigenvalues of F , i.e., $\hat{\lambda}_i = e^{\hat{\lambda}_i T_d}$, which gives $\tilde{\lambda}_i = \frac{\ln \hat{\lambda}_i}{T_d}$ for $i = 1, \dots, \tilde{n}$. The Koopman eigenvalues are solved as $\tilde{\lambda}_i = \frac{\ln \hat{\lambda}_i}{T_d}$, $i = 1, \dots, \tilde{n}$.

Back to the Hankel matrix $H_{\tilde{n}}(\tilde{X})$ (45), substituting the state decomposition (40) into (46) obtains $H_{\tilde{n}}(\tilde{X}) = Q_o \tilde{V} [\tilde{\varphi}(\tilde{X}(0)) \ \hat{\Lambda} \tilde{\varphi}(\tilde{X}(0)) \ \dots \ \hat{\Lambda}^{\tilde{n}-1} \tilde{\varphi}(\tilde{X}(0))] = Q_o \tilde{V} \text{diag}(\tilde{\varphi}_i(\tilde{X}(0))) V_F$, where $\text{diag}(\tilde{\varphi}_i(\tilde{X}(0)))$ is the diagonal matrix of initial eigenfunction values, and $V_F = (1_{\tilde{n}} \ \text{col}(\hat{\lambda}_i) \ \dots \ \text{col}(\hat{\lambda}_{\tilde{n}}^{\tilde{n}-1}))$. Especially, the Vandermonde matrix V_F is the inverse modal matrix of the companion matrix F , which implies that $V_F \tilde{\nu}_i = e_i$, where e_i is the i -th standard basis vector. Consequently, we can write

$$H_{\tilde{n}}(\tilde{X}) \tilde{\nu}_i = Q_o \tilde{V} \text{diag}(\tilde{\varphi}_i(\tilde{X}(0))) V_F \tilde{\nu}_i = \tilde{\varphi}_i(\tilde{X}(0)) Q_o \tilde{\nu}_i. \quad (\text{E.4})$$

Given the structure of the Q_o from (46) which he first block-row of $Q_o \tilde{\nu}_i$ is $\tilde{\nu}_i$ itself, and the constant $\tilde{\varphi}_i(\tilde{X}(0)) \neq 0, i = 1, \dots, \tilde{n}$, we isolate the Koopman modes as $\tilde{\nu}_i = [I_{\tilde{n}} \ 0] H_{\tilde{n}}(\tilde{X}) \tilde{\nu}_i, i = 1, \dots, \tilde{n}$. The proof is complete.

F. The proof of Lemma 6

Lemma 5 establishes that we can compute the Koopman operator eigenpairs from the measurement data using DMD. For the linear system (38) and observable \tilde{X} (40), Koopman function (39), Koopman eigenvalues and modes are also the eigenpairs of the system matrix \tilde{A} . Furthermore, Assumption 5 states that \tilde{A} is diagonalizable. Therefore, we exactly identify the system matrix \tilde{A} from the eigendecomposition obtained in Lemma 5 via (56). The estimated system parameters $\hat{\Theta}_1(D) = \{\mathcal{A}, \mathcal{S}_d, \tilde{\mathcal{G}}\}$ are then obtained by partitioning the reconstructed matrix \tilde{A} according to its block structure defined in (38), i.e., (53)–(55).

G. The proof of Lemma 8

For all $\tilde{\lambda} \in \text{eig}(S_d)$, it is obtained from Assumption 5 that the matrix $A - \tilde{\lambda}I$ is nonsingular. It allows the following rank calculation

$$\begin{aligned} & \text{rank} \begin{pmatrix} A - \tilde{\lambda}I & GP_d \\ C & 0 \end{pmatrix} \\ &= \text{rank} \begin{pmatrix} I & 0 \\ -C(A - \tilde{\lambda}I)^{-1} & I \end{pmatrix} \begin{pmatrix} A - \tilde{\lambda}I & GP_d \\ C & 0 \end{pmatrix} \\ &= \text{rank} \begin{pmatrix} A - \tilde{\lambda}I & GP_d \\ 0 & P_C(\tilde{\lambda}) \end{pmatrix} \end{aligned} \quad (\text{G.1})$$

where $P_C(\tilde{\lambda}) = -C(A - \tilde{\lambda}I)^{-1}GP_d \in \mathbb{R}^{1 \times n_d}$. It yields with (76) that $\text{rank } P_C(\tilde{\lambda}) = 1, \forall \tilde{\lambda} \in \text{eig}(S_d)$. Consider $C = [1, 0, \dots]$, we know that the first element of the vector $P_C(\tilde{\lambda})$ is not zero for all $\tilde{\lambda} \in \text{eig}(S_d)$. The eigenvectors of the companion matrix S_d (70) are of the form $v_{d,i} = (1, \tilde{\lambda}_i, \tilde{\lambda}_i^2, \dots, \tilde{\lambda}_i^n)^\top, i = 1, \dots, n_d$. It follows that $P_C(\tilde{\lambda}_i)v_{d,i} \neq 0, i = 1, \dots, n_d$. We further know from (41), (42) that $\bar{C}\tilde{v}_i \neq 0$, for $i = 1, \dots, n_d$. The observability of (C, A) and the PBH test ensure $C\nu_i \neq 0$, which implies $\bar{C}\tilde{v}_i = C\nu_i \neq 0$ for $i = n_d + 1, \dots, \tilde{n}$. Since $\bar{C}\tilde{v}_i \neq 0$ for all $i = 1, \dots, \tilde{n}$, the PBH test confirms that (\bar{C}, \bar{A}_d) is observable. It follows from Assumption 6 that (\bar{C}, \bar{A}_d) is observable as well. Consequently, the observability matrix Q_o in (75) has full rank, i.e., $\text{rank}(Q_o) = \tilde{n}$.

By the same argument as in the proof of Lemma 3, we have that $\text{rank } Q_c = \tilde{n}$. Since both Q_o and Q_c defined in (75), (47) are nonsingular, their product, the Hankel matrix $H_{\tilde{n}}(Y)$ (74), is also nonsingular and thus has full rank, i.e., (77).

H. The proof of Lemma 10

Follow the same process in the proof of Lemma 5, the result (80) is directly obtained.

According to Assumption 5 that all eigenvalues $\tilde{\lambda}_i$ are distinct, we can construct a Vandermonde matrix (82) from them, serving as the eigenvector matrix V_A for the companion matrix A . Combined with the diagonal matrix of eigenvalues $\Lambda_A = \text{diag}(\tilde{\lambda}_{n_d}, \dots, \tilde{\lambda}_{\tilde{n}})$, the matrix can be reconstructed using the formula $A = V_A \Lambda V_A^{-1}$. Similarly, we can reconstruct the disturbance matrix S_d using its eigenvalues $\tilde{\lambda}_i, i = 1, \dots, n_d$ and the corresponding Vandermonde matrix (82) as the eigenvector matrix V_d .

REFERENCES

- [1] A. D. Ames, J. W. Grizzle, and P. Tabuada, "Control barrier function based quadratic programs with application to adaptive cruise control," in *2014 IEEE 53rd Conference on Decision and Control (CDC)*. IEEE, 2014, pp. 6271–6278.
- [2] A. D. Ames, X. Xu, J. W. Grizzle, and P. Tabuada, "Control barrier function based quadratic programs for safety critical systems," *IEEE Trans. Autom. Control*, vol. 62, no. 8, pp. 3861–3876, 2017.
- [3] H. Anfinsen and O. M. Aamo, "Disturbance rejection in the interior domain of linear 2×2 hyperbolic systems," *IEEE Trans. Autom. Control*, vol. 60, no. 1, pp. 186–191, 2015.
- [4] H. Anfinsen and O. M. Aamo, "Model reference adaptive control of $n+1$ coupled linear hyperbolic PDEs," *Syst. Control Lett.*, vol. 109, pp. 1–11, 2017.
- [5] H. Arbabi and I. Mezić, "Ergodic theory, dynamic mode decomposition, and computation of spectral properties of the Koopman operator," *SIAM J. Appl. Dyn. Syst.*, vol. 16, no. 4, pp. 2096–2126, 2017.
- [6] A. S. Bazzanella, L. Campestrini, and D. Eckhard, *Data-driven controller design: The H_2 approach*. Springer Science & Business Media, 2011.
- [7] P. Bevanda, S. Sosnowski, and S. Hirche, "Koopman operator dynamical models: Learning, analysis and control," *Annu. Rev. Control*, vol. 52, pp. 197–212, 2021.
- [8] A. Bisoffi, C. De Persis, and P. Tesi, "Controller design for robust invariance from noisy data," *IEEE Trans. Autom. Control*, vol. 68, no. 1, pp. 636–643, 2022.
- [9] D. Bresch-Pietri and M. Krstic, "Adaptive trajectory tracking despite unknown input delay and plant parameters," *Automatica*, vol. 45, no. 9, pp. 2074–2081, 2009.
- [10] S. L. Brunton and J. N. Kutz, *Data-driven science and engineering: Machine learning, dynamical systems, and control*. Cambridge University Press, 2022.
- [11] C. De Persis and P. Tesi, "Formulas for data-driven control: Stabilization, optimality, and robustness," *IEEE Trans. Autom. Control*, vol. 65, no. 3, pp. 909–924, 2020.
- [12] J. Deutscher, "A backstepping approach to the output regulation of boundary controlled parabolic PDEs," *Automatica*, vol. 57, pp. 56–64, 2015.
- [13] J. Deutscher, "Backstepping design of robust state feedback regulators for linear 2×2 hyperbolic systems," *IEEE Trans. Autom. Control*, vol. 62, no. 10, pp. 5240–5247, 2017.
- [14] J. Deutscher, "Finite-time output regulation for linear 2×2 hyperbolic systems using backstepping," *Automatica*, vol. 75, pp. 54–62, 2017.
- [15] J. Deutscher, "Output regulation for general linear heterodirectional hyperbolic systems with spatially-varying coefficients," *Automatica*, vol. 85, pp. 34–42, 2017.
- [16] J. Deutscher, "Cooperative output regulation for a network of parabolic systems with varying parameters," *Automatica*, vol. 125, p. 109446, 2021.
- [17] J. Deutscher, "Data-driven robust output regulation of continuous-time LTI systems using Koopman operators," *IEEE Trans. Autom. Control*, vol. 69, no. 12, pp. 8774–8781, 2024.
- [18] J. Deutscher and J. Gabriel, "A backstepping approach to output regulation for coupled linear wave–ODE systems," *Automatica*, vol. 123, p. 109338, 2021.
- [19] Z. Drmac, I. Mezic, and R. Mohr, "Data driven modal decompositions: Analysis and enhancements," *SIAM J. Sci. Comput.*, vol. 40, no. 4, pp. A2253–A2285, 2018.
- [20] C. Folkestad, Y. Chen, A. D. Ames, and J. W. Burdick, "Data-driven safety-critical control: Synthesizing control barrier functions with Koopman operators," *IEEE Control Syst. Lett.*, vol. 5, no. 6, pp. 2012–2017, 2021.
- [21] B. A. Francis and W. M. Wonham, "The internal model principle of control theory," *Automatica*, vol. 12, no. 5, pp. 457–465, 1976.
- [22] W. Gao and Z.-P. Jiang, "Adaptive dynamic programming and adaptive optimal output regulation of linear systems," *IEEE Trans. Autom. Control*, vol. 61, no. 12, pp. 4164–4169, 2016.
- [23] Z.-S. Hou and Z. Wang, "From model-based control to data-driven control: Survey, classification and perspective," *Inform. Sciences*, vol. 235, pp. 3–35, 2013.
- [24] J. Huang, *Nonlinear output regulation: theory and applications*. SIAM, 2004.
- [25] J. Huang and Z. Chen, "A general framework for tackling the output regulation problem," *IEEE Trans. Autom. Control*, vol. 49, no. 12, pp. 2203–2218, 2004.
- [26] A. Irscheid, J. Deutscher, N. Gehring, and J. Rudolph, "Output regulation for general heterodirectional linear hyperbolic PDEs coupled with nonlinear ODEs," *Automatica*, vol. 148, p. 110748, 2023.
- [27] A. Isidori and C. I. Byrnes, "Output regulation of nonlinear systems," *IEEE Trans. Autom. Control*, vol. 35, no. 2, pp. 131–140, 1990.
- [28] M. Jankovic, "Robust control barrier functions for constrained stabilization of nonlinear systems," *Automatica*, vol. 96, pp. 359–367, 2018.
- [29] C. Johnson, "Further study of the linear regulator with disturbances—The case of vector disturbances satisfying a linear differential equation," *IEEE Trans. Autom. Control*, vol. 15, no. 2, pp. 2220–228, 1970.
- [30] S. Kolathaya and A. D. Ames, "Input-to-state safety with control barrier functions," *IEEE Control Syst. Lett.*, vol. 3, no. 1, pp. 108–113, 2019.
- [31] M. Krstic and M. Bement, "Nonovershooting control of strict-feedback nonlinear systems," *IEEE Trans. Autom. Control*, vol. 51, no. 12, pp. 1938–1943, 2006.

- [32] J. N. Kutz, S. L. Brunton, B. W. Brunton, and J. L. Proctor, *Dynamic mode decomposition: data-driven modeling of complex systems*. SIAM, 2016.
- [33] A. Mauroy, Y. Susuki, and I. Mezic, *Koopman operator in systems and control*. Springer, 2020, vol. 7.
- [34] T. Meurer and A. Kugi, “Tracking control for boundary controlled parabolic PDEs with varying parameters: Combining backstepping and differential flatness,” *Automatica*, vol. 45, no. 5, pp. 1182–1194, 2009.
- [35] I. Mezić, “Spectral properties of dynamical systems, model reduction and decompositions,” *Nonlinear Dynam.*, vol. 41, no. 1-3, pp. 309–325, 2005.
- [36] H. Modares, “Data-driven safe control of uncertain linear systems under aleatory uncertainty,” *IEEE Trans. Autom. Control*, vol. 69, no. 1, pp. 551–558, 2024.
- [37] T. G. Molnar, A. K. Kiss, A. D. Ames, and G. Orosz, “Safety-critical control with input delay in dynamic environment,” *IEEE Trans. Control Syst. Technol.*, vol. 31, no. 4, pp. 1507–1520, 2022.
- [38] Q. Nguyen and K. Sreenath, “Exponential control barrier functions for enforcing high relative-degree safety-critical constraints,” in *2016 American Control Conference (ACC)*. IEEE, 2016, pp. 322–328.
- [39] U. S. Park and M. Ikeda, “Stability analysis and control design of LTI discrete-time systems by the direct use of time series data,” *Automatica*, vol. 45, no. 5, pp. 1265–1271, 2009.
- [40] J. L. Proctor, S. L. Brunton, and J. N. Kutz, “Dynamic mode decomposition with control,” *SIAM J. Appl. Dyn. Syst.*, vol. 15, no. 1, pp. 142–161, 2016.
- [41] P. Rapisarda, M. K. Camlibel, and H. J. van Waarde, “A persistency of excitation condition for continuous-time systems,” *IEEE Control Syst. Lett.*, vol. 7, pp. 589–594, 2023.
- [42] J. Redaud, F. Bribiesca-Argomedo, and J. Auriol, “Output regulation and tracking for linear ODE-hyperbolic PDE-ODE systems,” *Automatica*, vol. 162, p. 111503, 2024.
- [43] A. J. Taylor and A. D. Ames, “Adaptive safety with control barrier functions,” in *2020 American Control Conference (ACC)*. IEEE, 2020, pp. 1399–1405.
- [44] H. L. Trentelman, H. J. van Waarde, and M. K. Camlibel, “An informativity approach to the data-driven algebraic regulator problem,” *IEEE Trans. Autom. Control*, vol. 67, no. 11, pp. 6227–6233, 2022.
- [45] H. J. van Waarde, J. Eising, H. L. Trentelman, and M. K. Camlibel, “Data informativity: A new perspective on data-driven analysis and control,” *IEEE Trans. Autom. Control*, vol. 65, no. 11, pp. 4753–4768, 2020.
- [46] J. Wang and M. Diagne, “Delay-adaptive boundary control of coupled hyperbolic PDE-ODE cascade systems,” *IEEE Trans. Autom. Control*, vol. 69, no. 12, pp. 8156–8171, 2024.
- [47] J. Wang and M. Krstic, “Output-positive adaptive control of hyperbolic PDE-ODE cascades,” *IEEE Trans. Autom. Control*, pp. 1–8, 2025.
- [48] J. Wang and M. Krstic, “Safe output regulation of coupled hyperbolic PDE-ODE system,” *arXiv preprint, arXiv:2512.05822v1*, 2025.
- [49] J. C. Willems, P. Rapisarda, I. Markovsky, and B. L. M. De Moor, “A note on persistency of excitation,” *Syst. Control Lett.*, vol. 54, no. 4, pp. 325–329, 2005.
- [50] W. Xiao and C. Belta, “High-order control barrier functions,” *IEEE Trans. Autom. Control*, vol. 67, no. 7, pp. 3655–3662, 2021.
- [51] Z. Zhao and J. Wang, “Safe delay-adaptive control of strict-feedback nonlinear systems with application in vehicle platooning,” *Automatica*, vol. 179, p. 112442, 2025.
- [52] L. Zhou, W. Liu, Y. Li, J. Sun, G. Wang, and L. Xie, “Robust data-driven control with safety constraints and fault detection,” *IEEE Trans. Autom. Control*, pp. 1–8, 2025.
- [53] L. Zhu and Z. Chen, “Data informativity for robust output regulation,” *IEEE Trans. Autom. Control*, vol. 69, no. 10, pp. 7075–7080, 2024.